Identification of Mebendazole as an ethylene signaling activator reveals a role of ethylene signaling in the regulation of lateral root angles

Wenrong He1, Hai An Truong 1, Ling Zhang 1, Min Cao 1, Neal Arakawa 3, Yao Xiao 4, Kaizhen Zhong1, Yingnan Hou 5, 6, Wolfgang Busch1,2,7

1. Plant Molecular and Cellular Biology Laboratory, Salk Institute for Biological Studies, La Jolla, California, USA
2. Integrative Biology Laboratory, Salk Institute for Biological Studies, La Jolla, California, USA
3. Environmental and Complex Analysis Laboratory (ECAL), Department of Chemistry and Biochemistry, University of California, San Diego, La Jolla, USA
4. Department of Integrative Structural and Computational Biology, The Scripps Research Institute, La Jolla, California, USA
5. Department of Microbiology and Plant Pathology, Center for Plant Cell Biology, University of California, Riverside, California, USA
6. School of Agriculture and Biology, Shanghai Jiao Tong University, Shanghai, China
7. Lead contact

Correspondence: wbusch@salk.edu

In brief: He et al. identify a small molecule that regulates lateral root angle. They show that the compound increases lateral root angle by inhibiting CTR1 kinase activity, which in turn activates ethylene signaling. Therefore, they uncover that the ethylene pathway is involved in lateral root angle regulation.

Highlights:

- MBZ increases lateral root angle
- MBZ regulates lateral root angle by activating ethylene signaling
- MBZ inhibits CTR1 kinase activity
- The ethylene pathway is involved in lateral root angle regulation

SUMMARY

The lateral root angle or gravitropic set-point angle (GSA) is an important trait for root system architecture (RSA) that determines the radial expansion of the root system. The GSA therefore plays a crucial role for the ability of plants to access nutrients and water in the soil. Despite its importance, only few regulatory pathways and mechanisms that determine GSA are known, and these mostly relate to auxin and cytokinin pathways. Here, we report the identification of a small molecule, Mebendazole (MBZ) that modulates GSA in *Arabidopsis thaliana* roots and acts via the activation of ethylene signaling. We uncover that MBZ directly acts on the serine/threonine protein kinase CTR1, which is a negative regulator of ethylene signaling. Our study not only reveals that the ethylene signaling pathway is essential for GSA regulation, but it also identifies a small molecular modulator of RSA and the first small molecule that acts downstream of ethylene receptors and that directly activates ethylene signaling.

KEYWORDS

Root System Architecture, Lateral Root Angle, Root Growth, Ethylene Signaling, Chemical genetics, Mebendazole

INTRODUCTION

The root systems of plants are vital for plant survival and productivity. They anchor plants and they absorb water and nutrients from the soil. The distribution of roots in the soil, root system architecture (RSA), is of enormous relevance. For instance, deeper rooting is associated with higher carbon permanence (Poirier et al., 2018), a critical trait for soil carbon sequestration and the ability of plants to survive terminal droughts (Uga et al., 2013). Besides, to enhance the capacity for root systems to efficiently uptake nitrogen and water, deeper roots are required, yet for improving the uptake of phosphate and other nutrients, shallower soil layers have to be accessed by roots (Lynch, 2019). A key determinant of RSA is the lateral root angle or gravitropic set-point angle (GSA). Previous studies have shown that auxin plays a crucial role in regulating GSA (Rosquete et al., 2013; Roychoudhry et al., 2013; Xiao and Zhang, 2020). Application of exogenous IAA

or synthetic auxin leads to lateral root growth toward the vector of gravity thereby decreasing GSA (Rosquete et al., 2013; Roychoudhry et al., 2013). Another phytohormone, cytokinin, was also found to be involved in the regulation of GSA. Application of cytokinin showed an anti-gravitropic effect and thereby increased GSA (Waidmann et al., 2019). Finally, members of the IGT gene family, including DRO1/LAZY4 have been shown to play a major role in lateral root angles via auxin associated mechanisms (Ge and Chen, 2016; Guseman et al., 2017; Waite and Dardick, 2021; Yoshihara and Spalding, 2017).

Ethylene is an ancient plant hormone whose signaling pathway is highly conserved and which has evolved in plants over 450 million years (Ju et al., 2015). Ethylene is produced from the conversion of S-adenosyl-L-methionine (SAM) to 1-aminocy-clopropane-1-carboxylic acid (ACC) and then to ethylene, which is catalyzed by enzymes including ACC synthase (ACS) and ACC oxidase (ACO) (Pattyn et al., 2021; S F Yang and Hoffman, 1984). When ethylene binds to its receptors (ETRs) (Chang et al., 1993; Hua et al., 1998; Sakai et al., 1998), it inactivates a serine/threonine protein kinase, CONSTITUTIVE TRIPLE RESPONSE1(CTR1) (Kieber et al., 1993). In the absence of ethylene, CTR1 blocks ethylene downstream responses by phosphorylating the C-terminal of ETHYLENE-INSENSITIVE2 (EIN2), an ER–associated membrane protein that works as a positive regulator of ethylene signaling (Alonso et al., 1999; Ju et al., 2012; Wen et al., 2012). This leads to the degradation of EIN2-CEND by the Ub/26S proteasome (Ju et al., 2012; Qiao et al., 2012a; Wen et al., 2012). When CTR1 is inactivated by ethylene binding to ETRs, EIN2-CEND is stabilized and moves into the nucleus to transduce the ethylene signal to downstream transcription factors, such as EIN3, EIN3 LIKE1 (EIL1) (An et al., 2010; Chao et al., 1997) and ETHYLENE RESPONSE FACTORs (ERFs) (Muller and Munne-Bosch, 2015). These transcription factors activate the downstream ethylene response. The ethylene pathway was found to play an important role in numerous growth and developmental processes in the root, such as the inhibition of root elongation (Kieber et al., 1993; Le et al., 2001; Vaseva et al., 2018), induction of root hair growth (Feng et al., 2017), and inhibition of the initiation of lateral roots (LRs) (Negi et al., 2008).

To identify potential regulators of GSA, we performed a chemical genetics screen and identified a small molecule, Mebendazole (MBZ), which dramatically increased GSA. Genetic analysis revealed that MBZ increased GSA through rapidly activating the ethylene signaling pathway. Both MBZ and ACC treatment induced ethylene signaling, which led to a modulation of lateral root angle. Further molecular and biochemistry studies showed that MBZ activates ethylene signaling by specifically targeting CTR1 and thereby blocking its kinase activity. Our study not only identified MBZ as an efficient small molecular activator of ethylene signaling, but also uncovered that ethylene signaling plays an important role in regulating GSA.

Results

A small compound profoundly affects the lateral root gravitropic set-point angle (GSA) in Arabidopsis

To identify small molecules that affect GSA, we screened chemicals for their ability to change GSA of young seedlings from a small molecular library with 2000 diverse generic chemicals (SP 2000)(He et al., 2011; Sun et al., 2017; Zhu et al., 2019). We found that treatment with Mebendazole (MBZ) (Figure S1A) led to a distinct increase of lateral root angles that caused lateral roots to grow in a more horizontal direction (Figure 1A). The lateral root GSA of untreated two-week-old Arabidopsis seedlings was approx. 46°, and the GSA of lateral roots of seedlings grown on 1 µM MBZ plates was approx. 70° (Figure 1A, B). While the lateral root angle was the most striking phenotype, at a much earlier developmental stage (one week after germination), seedlings on 1 µM MBZ displayed a decreased root length (in average reduced by 37%) and an increased root hair initiation and elongation (Figure 1C, D, Figure S1B, C). To test how quickly MBZ would affect lateral root growth, we grew seedlings for 14 days on ½ MS medium with DMSO, then transferred them to ½ MS medium supplemented with 1 µM MBZ and acquired images every 10 minutes. All of the 5 measured lateral root tips started to grow at a more horizontal (less steep) angle within 3 hours of MBZ treatment (Figure 1E upper panel, F), which coincided with the first timepoint at which root angles were significantly different between control and MBZ (Welch Two Sample t-test; p-value <0.05). To test whether the action of MBZ was reversible, we germinated and grew seedlings on ½ MS for 5 days,

and then transferred them to medium containing 1 µM MBZ for 14 days, thereby inducing lateral roots of MBZ treated seedlings to grow more horizontal. We note that we used this later timepoint (compared to the data presented in the upper panel) to be able to consider enough lateral roots that were growing at the more horizontal angle. We then transferred the seedlings back to control conditions and acquired images every 10 minutes. Already after one hour root angles was significantly different between control (MBZ) and treatment (removal from MBZ) conditions (Welch Two Sample t-test; p-value <0.05), and within 4 hours all 5 lateral root tips we measured started to grow at a distinctly steeper angle upon removal from MBZ (Figure 1E bottom panel, F). These data showed that the treatment of Arabidopsis roots with MBZ changes lateral root angles within 3 hours and that this effect is fully reversible. In summary, we found that MBZ changes lateral root angles, and important RSA traits associated with the development of a shallow root system.

Application of MBZ induces the ethylene pathway

To identify the pathway that MBZ acted upon, we utilized a genome-scale expression profiling approach. For this, we performed an mRNA-seq experiment using whole roots of 14-days-old Arabidopsis grown on ½ MS media treated with 10 µM MBZ for 4 hours. The analysis revealed that 677 genes were induced compared to mock treatment (FDR<0.05; log2 fold change > 1) and 658 genes were repressed (FDR<0.05; log2 fold change < -1). A gene ontology (GO) analysis revealed that among the genes that were upregulated by MBZ, genes involved in ethylene responses were strongly overrepresented in this early response. In particular, the GO process “negative regulation of ethylene-activated signaling pathway” (GO:0010105) was the most enriched process (~21 fold enrichment, P-value: $6.07*10^{-4}$) upon MBZ treatment (Figure 2A), and the 4th most enriched GO process was “ethylene-activated signaling pathway” (GO:0009873) (~11 fold enrichment, P-value:$7.45*10^{-5}$) (Figure 2A). Other GO categories were also significantly enriched, most notably responses to light. However, given that ethylene signaling was the most enriched GO term, we first looked at the responses of genes involved in the ethylene hormone pathway. A major portion of these genes were differentially regulated by MBZ compared to mock treatment (Figure 2A, B). We therefore hypothesized that MBZ elicited the ethylene pathway. To test this hypothesis, we first

compared the set of genes that had responded to MBZ with a published transcriptome dataset that had been generated by exposing roots to 4 hours of ethylene treatment(Chang et al., 2013). Of the 1335 differentially expressed genes (DEGs) upon the 4 hours of MBZ treatment, 306 were overlapping with 1397 DEGs upon 4 hours of ethylene treatment (P-value for the overlap using a hypergeometric test: $p < 4.657*10^{-143}$) (Figure S3A). Notably, more than 90% of these common DEGs retained the directionality of their expression change (i.e. genes upregulated by MBZ were also upregulated by ethylene treatment and vice versa) (Figure S3B, C). While this overlap was highly significant and supported the hypothesis that MBZ elicited ethylene responses, there was a high number of differentially expressed genes that didn't overlap. We reasoned that this might be due to differences in developmental and growth conditions of our MBZ treated plants and of those plants used for the published ethylene treatment dataset. For instance, we had used grown seedlings for 14-day-old seedlings under long day conditions before we conducted the treatment and the published data had utilized 3-day-old, dark grown seedlings for eliciting the classical ethylene triple response phenotype. To compare ethylene responses to MBZ responses under the same growth conditions and plant age, we performed another mRNA-seq experiment using roots of 14-days-old Arabidopsis grown on ½ MS media treated with 10 µM MBZ or 10 µM ACC (the ethylene precursor) for 3 hours. We then again compared the overlap of the responsive genes. Out of 826 differentially expressed genes (DEGs)(FDR < 0.05; abs(log2) fold change > 1) upon the MBZ treatment, 524 were overlapping with 741 DEGs)(FDR < 0.05; abs(log2) fold change > 1) upon 3 hours of ACC treatment, accounting for 63 and 71% of DEGs upon MBZ and ACC treatment respectively (Figure 2C). 77% upregulated DEGs (FDR < 0.05; log2 fold change > 1) of the MBZ treatment overlapped with 65% upregulated DEGs (FDR < 0.05; log2 fold change > 1) of the ACC treatment (Figure 2D). These fractions were 54% and 75% for downregulated DEGs (FDR < 0.05; log2 fold change < -1) (Figure 2E). Taken together, our data strongly suggested that application of MBZ induces the ethylene pathway.

MBZ induces ethylene responses

To investigate how MBZ treatment acts upon the ethylene response, we compared plant responses to MBZ and the ethylene precursor ACC. The most characteristic response to ethylene treatment is the triple response of etiolated seedlings (Guzman and Ecker, 1990) (Figure 3A to C), which includes shortened and thickened roots and hypocotyls, and an exaggerated apical hook. Consistent with our hypothesis that MBZ activates ethylene responses, 3-day-old etiolated seedlings treated with 10 µM MBZ showed a significant triple response phenotype (Figure 3A to C). Using different doses of MBZ, we found that 2.5 µM of MBZ was sufficient to induce the triple response phenotype in a dark environment (Figure S3A to F), we therefore started to use 2.5 µM of MBZ to observe triple responses. Consistent with MBZ mimicking ethylene treatment, MBZ induced triple response was abolished in the ethylene insensitive mutants *ein2-5* and *ein3 eil1* (Figure S3D to F). Ethylene treatment inhibits root elongation mainly by repressing cell elongation instead of the length of meristem (De Cnodder et al., 2005; Vaseva et al., 2018). We therefore measured the length of root cells of 4-day-old etiolated seedlings treated with 2.5 µM MBZ and 10 µM ACC, and found that similar to the ACC treatment, the mature cell size was reduced by MBZ treatment (Figure 3D to F). Altogether, our data strongly suggested that MBZ elicits its effects via the ethylene pathway.

As we wanted to identify the mechanism by which MBZ changes the steepness of lateral root angles and given our data that MBZ acts on the ethylene pathway, we conducted an RNA-seq experiment on lateral root tips that had been treated either with DMSO or MBZ for 3 hours. As sample collection was very challenging and took an hour per replicate, the sampled lateral roots had been treated for a time between 3-4 hours. The most enriched gene ontology categories were “regulation of transcription”, “response to auxin”, “ethylene activated signaling pathway” and “cytokinin-signaling pathway" (Figure 2F). Given the that the time window for the RNA-seq coincided with the change of lateral root angle, it was not surprising to detect auxin and cytokinin, as these two hormonal pathways had been shown to be involved in determining the GSA of lateral roots (Rosquete et al., 2013; Roychoudhry et al., 2013; Waidmann et al., 2019). However, given the occurrence of these pathways we wanted to check whether these pathways are activated before or after ethylene responses were elicited by MBZ. To do this, we obtained the *DR5-GFP V2* auxin response reporter line (Liao et al., 2015), the *35S-EIN3-GFP* ethylene reporter line in the

ein3 eil1 background (He et al., 2011), and the *TCN-GFP* cytokinin reporter line (Zurcher et al., 2013) We then conducted time-lapse spinning disk confocal microscopy on lateral root tips that were either treated with a DMSO control solution, MBZ, or the respective positive control (the auxin IAA, the cytokinin Zeatin, or the ethylene precursor ACC). All positive control treatments swiftly induced the expression of the reporter genes in lateral roots (Figure 2G-L; Suppl. Movies 1, 3, 4, 6, 7, 9). Consistent with our hypothesis that MBZ induced the ethylene pathway, MBZ treatment drastically induced the ethylene reporter within the first 20 minutes after treatment, even before the ethylene precursor ACC induced the reporter (Figure 2G, J; Suppl. Movies 1-3). MBZ also very slightly induced the auxin response reporter after 40 minutes, but at a much lower level than the positive control (Figure 2H, K; Suppl. Movies 4-6). There was no induction of the cytokinin reporter by MBZ in the timeframe we observed the roots (Figure 2I, L; Suppl. Movies 7-9). Overall, these data strongly suggested that MBZ strongly and swiftly induces the ethylene pathway in lateral root tips.

MBZ actives ethylene signaling

Next, we set out to locate the target of MBZ in the ethylene pathway. First, we tested whether MBZ induces ethylene biosynthesis, or acts on the perception of ethylene, or on the ethylene signaling pathway. To test whether ethylene biosynthesis is affected, we measured ethylene production by GC-MS in 3-days-old etiolated Col-0 seedlings that were treated with 10 µM MBZ or ACC. Ethylene production was dramatically induced by 10 µM ACC, but not detected in DMSO or 10 µM MBZ treated seedlings (Figure 4A). The results suggested that MBZ acts downstream of ethylene biosynthesis. To further test this hypothesis, we utilized the *etr1,* ethylene receptor mutants. Root growth and GSA in mutants with strong alleles of *etr1*, *etr1-1* and *etr1-3* were still strongly altered upon MBZ treatment (Figure 4B to E). Moreover, 4-days-old etiolated seedlings of *etr1-3* treated with 2.5 µM MBZ showed the typical triple response phenotype, demonstrating that ethylene responses are triggered by MBZ even without induced ethylene production or the perception of ethylene by ETR1. In contrast to the response to MBZ, *etr1-3* plants were completely insensitive to the treatment with 10 µM of ACC (Figure S3A to C). Collectively,

these results show that MBZ induces ethylene responses by targeting factors downstream of ethylene biosynthesis and perception.

To uncover which components of ethylene signaling are targeted by MBZ, we studied MBZ responses in key mutants of the ethylene signaling pathway. First, we checked the root inhibition phenotype and GSA in *ctr1-1* mutant treated with MBZ and compared these responses to the Col-0 wild type. *CTR1* is the first negative regulator of ethylene signaling that downstream of receptors, and *EIN2* and *EIN3/EIL1* act downstream of *CTR1* to trigger ethylene signaling. (Figure 5A). Roots of Col-0 were sensitive to 1.2 µM MBZ treatment and showed short roots and increased root hair development (Figure 5B, C). However, *ctr1-1* mutants in which ethylene signaling is constitutively active, showed short roots and abundant root hairs without any treatment at an early stage. Due to this pronounced early-seedling phenotype, we could not confidently assess changes in response to MBZ. However, we noticed that root growth remained insensitive to MBZ (Figure 5B, C). We further measured GSA at a later stage of development, which we had found to be a major effect of MBZ treatment. 3-week-old *ctr1-1* plants were insensitive to MBZ with regards to GSA (Figure 5D, E). Interestingly, *ctr1-1* without MBZ treatment, showed an increased lateral root angle phenotype, which mimics MBZ treatment, suggesting that CTR1 might be the target of MBZ in ethylene signaling. Consistent with this hypothesis, root growth and GSA of *ein2-5* and *ein3 eil1* were clearly not affected by MBZ treatment (Figure 5B, C, F, G) and in fact, *ein2-5* mutant plants, which are insensitive to ethylene, displayed steeper lateral root angles under control conditions compared to the wildtype (Figure 5F, G). We further tested triple responses in *ctr1-1*, *ein2-5* and *ein3 eil1* mutants. Consistent with the observation of root inhibition and GSA in *ctr1-1*, these plants showed a constitutive triple response regardless of MBZ treatment. *ein2-5* and *ein3 eil1* plants were also insensitive to MBZ treatment (Figure S3D to F). Taken together our data showed that MBZ activates ethylene signaling most likely by interfering with CTR1 in the ethylene signaling pathway.

MBZ is a potent inhibitor of CTR1 kinase activity

To pinpoint whether CTR1 is the target of MBZ, we capitalized on what is known about the activity of MBZ in mammalian systems. There, MBZ has been reported to be an

inhibitor of the serine/threonine kinase *homo sapiens* (*hs*) MAPK14 (Ariey-Bonnet et al., 2020). Because CTR1 is also a serine/threonine protein kinase (Kieber et al., 1993), we hypothesized that CTR1 is the direct target of MBZ in plants. Since it was shown that there are 4 critical amino acid residues in the catalytic site of *hs*MAPK14 that are relevant for MBZ binding (Ariey-Bonnet et al., 2020), we first tested *in silico* whether these residues were conserved between *hs*MAPK14 and CTR1. For this, we aligned the amino-acid sequence of the Arabidopsis CTR1 and *hs*MAPK14 kinase domains (Figure 6A, Figure S4A, B). We found 3 (Lys 578, Thr 625, and Asp 694) of the 4 critical amino acid residues were conserved between the CTR1 kinase domain and that of *hs*MAPK14 (Figure 6A). The 4th critical residue is Met 109 in *hs*MAPK14, which corresponds to Leu 628 in CTR1. Because both Met and Leu are non-polar amino acids with hydrophobic side chains and similar structure, it appeared possible that the replacement of Met by Leu in the CTR1 kinase domain does not significantly change the pocket structure for MBZ binding. We therefore hypothesized that the kinase domains of CTR1 and MAPK14 might have similar structures and function with regards to binding MBZ (Figure S4B).

To test this hypothesis, we first performed an *in silico* docking analysis using the published crystal structures of CTR1 (Mayerhofer et al., 2012)(PDB: 3PPZ) and MBZ (CHEMBL685). We found that MBZ is predicted to bind into the pocket of the CTR1 kinase domain (Figure 6B) formed by the aforementioned key amino acids (Figure 6A, B, Figure S4B). Overall, these analyses indicated that CTR1 could be the target of MBZ in Arabidopsis.

To further test this model, we expressed the recombinant kinase domains (KD) of CTR1 and MAPK4 (a MAPK protein in Arabidopsis with a highly similar amino acid sequence to *hs*MAPK14) (Table S1, Figure S4C, D). We then confirmed the kinase inhibitory activity of MBZ through an *in vitro* phosphorylation assay via anti-Thiophosphate-Ester antibodies (Allen et al., 2007). Using the phosphorylation state of MBP (substrate) as the readout of the kinase activity, we found that MBZ inhibited the kinase activities of both CTR1-KD and MPK4 in a concentration dependent manner, however, the inhibition for CTR1-KD was much more pronounced (Figure 6C, D). In particular, 10 µM MBZ strongly inhibited the kinase activity of CTR1-KD, while 100 µM MBZ totally blocked its activity. This assay demonstrated that MBZ can directly inhibit the kinase activity of CTR1-KD. Together with our genetic data that *ctr1-1* mutant mimicked the effect of MBZ on GSA and the triple

response phenotypes (Figure 5D, E, Figure S3D-F), and our molecular docking data (Figure 6B), our data strongly suggest that CTR1 is a direct target of MBZ in Arabidopsis. Taken together, our data support a model in which MBZ is a small molecular inhibitor of the CTR1 kinase activity and thereby triggers the ethylene signaling pathway by permitting C-terminal of EIN2 (EIN2C) translocation into the nucleus, which in turn triggers ethylene downstream responses (Figure 7A, B).

DISCUSSION

Our chemical genetic screen led to the identification of MBZ as a potent inhibitor of the kinase activity of CTR1, which is a negative modulator of the ethylene signaling pathway (Figure 7B). MBZ therefore is an activator of ethylene signaling, and to our knowledge the first small molecule that acts downstream of ethylene receptors and that directly activates ethylene signaling. In previous studies, ethylene gas and ACC have been used to activate the ethylene signaling pathway. However, there were notable disadvantages to use these approaches. In the case of treatment with ethylene gas, it is difficult to maintain a continuous treatment over longer periods of time due to the technical challenges for constantly maintaining the required ethylene concentrations. Because its controlled application is technically less challenging, ACC has been used more widely to study the role of ethylene. However, ACC was recently found to be a signaling molecule which can act independently of the ethylene pathway (Mou et al., 2020). Moreover, the necessity for enzymatic ACC conversion to ethylene in plants might be limiting in different tissues or conditions. Consequently, a direct activator of the ethylene signaling pathway such as MBZ promises to be an enormously useful tool for the field. Such tools have been lacking so far despite a number of attempts that have been made to identify small molecular regulators of ethylene signaling. Neither approaches targeting ethylene biogenesis and perception, nor approaches targeting downstream auxin biosynthesis had yielded in molecules acting on ethylene signaling (He et al., 2011; Li et al., 2017; Sun et al., 2017; Zhu et al., 2019).

Because CTR1 contains the critical MBZ binding residues that had been elucidated in the human MBZ target *hs*MPK14, and because of the profound genetic evidence for CTR1,

it is somewhat unlikely that other components in the ethylene pathway such as the E3 ligases ETP1/2 and EBF1/2, which negatively regulate EIN2 and EIN3 respectively (Guo and Ecker, 2003; Qiao et al., 2012b), are targets of MBZ. Another signaling pathway that impinges on ethylene signaling is the glucose-activated TOR signaling pathway, which had recently been shown to regulate EIN2 activity through phosphorylation (Fu et al., 2021). However, the TOR kinase does not contain any of the 4 key residues known for MBZ binding. Moreover, unlike MBZ, none of the inhibitors of TOR, including Rap, Torin2, and AMA, did induce the ethylene induced triple response phenotype (Fu et al., Nature 2021). In addition, *ein2-5* and *ein3 eil1* mutants displayed a shorter hypocotyl when the Glu-TOR-EIN2 pathway was inhibited (Fu et al Nature 2021, Figure 1b), but these mutants did not respond to MBZ treatment (Figure S3D, E). Altogether, it is most likely that the observed response of MBZ on the ethylene signaling is exerted via its binding to CTR1.

While most of the effects of MBZ are related to its activation of ethylene signaling, our RNA profiling indicated additional effects of MBZ. Consistently, treatment with high concentration of MBZ or long-term treatment with it, led to strongly inhibited plant growth and development, including a disrupted root apical meristem and morphological changes of leaves. These phenotypes have not been observed upon ethylene treatment (Figure S5A, B), raising the possibility that MBZ may have other targets in plants. MAPK4 has the highest amino acid sequence similarity to the human MBZ target *hs*MAPK14 (Table S1). Compared to CTR1, the effect of MBZ on MAPK4 kinase activity was much less pronounced (Figure 6C), consistent with the lack of conservation of key amino acids relevant for MBZ binding (Figure S4C). Although MBZ couldn't inhibit the kinase activity of MAPK4 as strongly as that of CTR1-KD, a decrease of the weak MAPK4 autophosphorylation band might indicate that MBZ treatment can disrupt MAPK4 autophosphorylation (Figure 6C). This raises the possibility that MBZ might alter autophosphorylation of MAPK4 and probably other CTR1-like kinases, based on the sequence conservation of the 4 critical residues (Figure 6A, Figure S4B). This might explain the additional effects of MBZ. Additionally, there are a number of CTR1 paralogs in Arabidopsis. This includes the kinases encoded by AT4G24480, AT1G08720,

At1g18160, AT1G67920, and AT5G11850. These kinases contain all 4 critical amino acids, raising the possibility that MBZ may also bind to these paralogs. Another explanation for the observed effects of MBZ that go beyond observed ethylene effects, might be that continuous activation of ethylene signaling via CTR1 might have more complicated or compounded effects than are elicited by external ethylene or ACC treatment (Figure S5C). Support for this comes from the *ctr1-1* mutant, which is dwarfed and shows aberration in leaf forms and thereby displays much stronger phenotypes than elicited with ACC or ethylene treatment (Kieber et al., 1993) (Figure 5B, D, Figure S5C). While MBZ's predominant effect on ethylene signaling via CTR1 is strongly supported by our study, further studies will be needed to elucidate the details of MBZ specificity.

One of the most intriguing effects of MBZ on the plant is its potent ability to change GSA. This suggests that ethylene signaling is involved in the regulation of the gravitropic setpoint angle in lateral roots. While important regulatory roles for GSA are known for auxin and cytokinin, and there can be complex interplays between auxin, cytokinin and ethylene, the induction of the ethylene signaling pathway clearly dominated responses in lateral roots after they were treated with MBZ (Figure 2). This activation of the ethylene responses occurred before angles of lateral roots were changing and was maintained throughout the timescale at which GSA was changed by the MBZ treatment, which occurred after 1-4 hours of MBZ treatment (Figure 1E, F, Figure 2, Figure S2I). In our study, we found that MBZ didn't induce ethylene biosynthesis (Figure 4A). ACC treatment had a weak but distinct effect on root angle and displayed concentration-dependent effects when applying a large range of concentrations (Figure S5C). Strong direct evidence for the impact of ethylene signaling in regulating lateral root set point angle is provided by the RSA phenotype of the *ctr1-1* mutant. In *ctr1-1*, ethylene signaling is constitutively activated and leads to an increased lateral root angle (Figure 5D, E). Conversely, we observed that the ethylene insensitive *ein2-5* mutant displays steeper lateral roots (Figure 5F, G). Overall, this exposes a yet unknown role of ethylene signaling in the regulation of lateral root set point angle. One reason why the role of ethylene in the regulation of lateral root angles hasn't been recognized so far might be that it reduces lateral root formation by itself (Negi et al., 2008) making the study of lateral root angles

more difficult. Our study strongly suggests that it will be worthwhile to explore the role of ethylene and its interaction with auxin and cytokinin in root gravitropism and RSA. Moreover, MBZ might also be used as a versatile tool for exploring the molecular mechanisms of root gravitropism and lateral root set point angles since as a small molecule, and due to its reversible mode of action, it can be easily applied to elicit controlled changes of lateral root angles. It might also be useful to reveal the mechanisms underlying GSA regulation by phytohormones and known GSA signals, such as the *LAZY* family genes (Furutani and Morita, 2021). Finally, since ethylene signaling is a widely conserved process in land plants, exploring the ability of MBZ or genetic perturbation of the ethylene pathway to change RSA in crop species might be highly worthwhile for RSA engineering.

Acknowledgements

The research was supported by start-up funds from the Salk Institute for Biological Studies and funds from the Harnessing Plants Initiative to WB, a Salk Women & Science Special Award and a Pioneer Fund Postdoctoral Scholar Award to WH. We are grateful to Dr. Glenn R. Hicks and Dr. Natasha Raikhel for sharing the SP2000 small molecule library. We thank Dr. Cris Argueso and Dr. Dolf Weijers for sharing seeds. We also thank Dr. Joseph R. Ecker and Dr. Joanne Chory for critical discussions. We thank the Next Generation Sequencing Core of Salk institute for NGS Library preparation & sequencing. We also thank Matthieu Platre, Nicole Gibbs, Anna Malolepszy, Björn Willige and Travis Lee for fruitful discussions and suggestions.

Author contributions

Wenrong He and Wolfgang Busch conceived the project and the experiments. Wenrong He performed the SP2000 library screen and analysis with help from Yingnan Hou. Wenrong He performed the phenotyping, qPCR, alignment, docking, protein purification, kinase activity assay. Wenrong He conducted the microscopy and mRNA-seq on primary roots with help from Kaizhen Zhong. Hai An Truong performed the time lapse reporter analysis using spinning disk microscopy, as well as the whole root system and lateral root RNA-seq experiments. Ling Zhang conducted the mRNA-seq analysis and the statistical analysis. Wenrong He conducted heatmap analysis of mRNA-seq. Wenrong He and Ling Zhang conducted Gene ontology analysis. Min Cao provided the protocol and suggestions for kinase activity assay. Neal Arakawa performed the GC test. Yao Xiao

performed the FPLC. Wenrong He and Wolfgang Busch wrote the manuscript with input from all authors. Wolfgang Busch provided materials, funding, supervision, guidance and advice on the project, the experiments, and the analysis of the results.

References

Allen, J.J., Li, M., Brinkworth, C.S., Paulson, J.L., Wang, D., Hubner, A., Chou, W.H., Davis, R.J., Burlingame, A.L., Messing, R.O.*, et al.* (2007). A semisynthetic epitope for kinase substrates. Nat Methods *4*, 511-516.

Alonso, J.M., Hirayama, T., Roman, G., Nourizadeh, S., and Ecker, J.R. (1999). EIN2, a bifunctional transducer of ethylene and stress responses in Arabidopsis. Science *284*, 2148-2152.

An, F., Zhao, Q., Ji, Y., Li, W., Jiang, Z., Yu, X., Zhang, C., Han, Y., He, W., Liu, Y.*, et al.* (2010). Ethylene-induced stabilization of ETHYLENE INSENSITIVE3 and EIN3-LIKE1 is mediated by proteasomal degradation of EIN3 binding F-box 1 and 2 that requires EIN2 in Arabidopsis. Plant Cell *22*, 2384-2401.

Ariey-Bonnet, J., Carrasco, K., Le Grand, M., Hoffer, L., Betzi, S., Feracci, M., Tsvetkov, P., Devred, F., Collette, Y., Morelli, X.*, et al.* (2020). In silico molecular target prediction unveils mebendazole as a potent MAPK14 inhibitor. Mol Oncol *14*, 3083-3099.

Chang, C., Kwok, S.F., Bleecker, A.B., and Meyerowitz, E.M. (1993). Arabidopsis ethylene-response gene ETR1: similarity of product to two-component regulators. Science *262*, 539-544.

Chang, K.N., Zhong, S., Weirauch, M.T., Hon, G., Pelizzola, M., Li, H., Huang, S.S.C., Schmitz, R.J., Urich, M.A., Kuo, D.*, et al.* (2013). Temporal transcriptional response to ethylene gas drives growth hormone cross-regulation in Arabidopsis. Elife *2*.

Chao, Q., Rothenberg, M., Solano, R., Roman, G., Terzaghi, W., and Ecker, J.R. (1997). Activation of the ethylene gas response pathway in Arabidopsis by the nuclear protein ETHYLENE-INSENSITIVE3 and related proteins. Cell *89*, 1133-1144.

De Cnodder, T., Vissenberg, K., Van Der Straeten, D., and Verbelen, J.P. (2005). Regulation of cell length in the Arabidopsis thaliana root by the ethylene precursor 1-aminocyclopropane- 1-carboxylic acid: a matter of apoplastic reactions. The New phytologist *168*, 541-550.

Feng, Y., Xu, P., Li, B., Li, P., Wen, X., An, F., Gong, Y., Xin, Y., Zhu, Z., Wang, Y.*, et al.* (2017). Ethylene promotes root hair growth through coordinated EIN3/EIL1 and RHD6/RSL1 activity in Arabidopsis. Proc Natl Acad Sci U S A *114*, 13834-13839.

Fu, L.W., Liu, Y.L., Qin, G.C., Wu, P., Zi, H.L., Xu, Z.T., Zhao, X.D., Wang, Y., Li, Y.X., Yang, S.H.*, et al.* (2021). The TOR-EIN2 axis mediates nuclear signalling to modulate plant growth. Nature *591*, 288-+.

Furutani, M., and Morita, M.T. (2021). LAZY1-LIKE-mediated gravity signaling pathway in root gravitropic set-point angle control. Plant Physiology *187*, 1087-1095.

Ge, L.F., and Chen, R.J. (2016). Negative gravitropism in plant roots. Nature plants *2*.

Guo, H., and Ecker, J.R. (2003). Plant responses to ethylene gas are mediated by SCF(EBF1/EBF2)-dependent proteolysis of EIN3 transcription factor. Cell *115*, 667-677.

Guseman, J.M., Webb, K., Srinivasan, C., and Dardick, C. (2017). DRO1 influences root system architecture in Arabidopsis and Prunus species. Plant J *89*, 1093-1105.

Guzman, P., and Ecker, J.R. (1990). Exploiting the triple response of Arabidopsis to identify ethylene-related mutants. Plant Cell *2*, 513-523.

He, W.R., Brumos, J., Li, H.J., Ji, Y.S., Ke, M., Gong, X.Q., Zeng, Q.L., Li, W.Y., Zhang, X.Y., An, F.Y., *et al.* (2011). A Small-Molecule Screen Identifies L-Kynurenine as a Competitive Inhibitor of TAA1/TAR Activity in Ethylene-Directed Auxin Biosynthesis and Root Growth in Arabidopsis. Plant Cell *23*, 3944-3960.

Hua, J., Sakai, H., Nourizadeh, S., Chen, Q.G., Bleecker, A.B., Ecker, J.R., and Meyerowitz, E.M. (1998). EIN4 and ERS2 are members of the putative ethylene receptor gene family in Arabidopsis. Plant Cell *10*, 1321-1332.

Ju, C., Van de Poel, B., Cooper, E.D., Thierer, J.H., Gibbons, T.R., Delwiche, C.F., and Chang, C. (2015). Conservation of ethylene as a plant hormone over 450 million years of evolution. Nature plants *1*, 14004.

Ju, C., Yoon, G.M., Shemansky, J.M., Lin, D.Y., Ying, Z.I., Chang, J., Garrett, W.M., Kessenbrock, M., Groth, G., Tucker, M.L., *et al.* (2012). CTR1 phosphorylates the central regulator EIN2 to control ethylene hormone signaling from the ER membrane to the nucleus in Arabidopsis. Proc Natl Acad Sci U S A *109*, 19486-19491.

Kieber, J.J., Rothenberg, M., Roman, G., Feldmann, K.A., and Ecker, J.R. (1993). CTR1, a negative regulator of the ethylene response pathway in Arabidopsis, encodes a member of the raf family of protein kinases. Cell *72*, 427-441.

Le, J., Vandenbussche, F., Van Der Straeten, D., and Verbelen, J.P. (2001). In the early response of Arabidopsis roots to ethylene, cell elongation is up- and down-regulated and uncoupled from differentiation. Plant Physiol *125*, 519-522.

Li, W., Lacey, R.F., Ye, Y., Lu, J., Yeh, K.C., Xiao, Y., Li, L., Wen, C.K., Binder, B.M., and Zhao, Y. (2017). Triplin, a small molecule, reveals copper ion transport in ethylene signaling from ATX1 to RAN1. PLoS Genet *13*, e1006703.

Liao, C.Y., Smet, W., Brunoud, G., Yoshida, S., Vernoux, T., and Weijers, D. (2015). Reporters for sensitive and quantitative measurement of auxin response. Nat Methods *12*, 207-210, 202 p following 210.

Lynch, J.P. (2019). Root phenotypes for improved nutrient capture: an underexploited opportunity for global agriculture. New Phytol *223*, 548-564.

Mayerhofer, H., Panneerselvam, S., and Mueller-Dieckmann, J. (2012). Protein kinase domain of CTR1 from Arabidopsis thaliana promotes ethylene receptor cross talk. J Mol Biol *415*, 768-779.

Mou, W., Kao, Y.T., Michard, E., Simon, A.A., Li, D., Wudick, M.M., Lizzio, M.A., Feijo, J.A., and Chang, C. (2020). Ethylene-independent signaling by the ethylene precursor ACC in Arabidopsis ovular pollen tube attraction. Nat Commun *11*, 4082.

Muller, M., and Munne-Bosch, S. (2015). Ethylene Response Factors: A Key Regulatory Hub in Hormone and Stress Signaling. Plant Physiol *169*, 32-41.

Negi, S., Ivanchenko, M.G., and Muday, G.K. (2008). Ethylene regulates lateral root formation and auxin transport in Arabidopsis thaliana. Plant J *55*, 175-187.

Pattyn, J., Vaughan-Hirsch, J., and Van de Poel, B. (2021). The regulation of ethylene biosynthesis: a complex multilevel control circuitry. New Phytol *229*, 770-782.

Poirier, V., Roumet, C., and Munson, A.D. (2018). The root of the matter: Linking root traits and soil organic matter stabilization processes. Soil Biology and Biochemistry *120*, 246-259.

Qiao, H., Shen, Z., Huang, S.S., Schmitz, R.J., Urich, M.A., Briggs, S.P., and Ecker, J.R. (2012a). Processing and subcellular trafficking of ER-tethered EIN2 control response to ethylene gas. Science *338*, 390-393.

Qiao, H., Shen, Z.X., Huang, S.S.C., Schmitz, R.J., Urich, M.A., Briggs, S.P., and Ecker, J.R. (2012b). Processing and Subcellular Trafficking of ER-Tethered EIN2 Control Response to Ethylene Gas. Science *338*, 390-393.

Rosquete, M.R., von Wangenheim, D., Marhavy, P., Barbez, E., Stelzer, E.H., Benkova, E., Maizel, A., and Kleine-Vehn, J. (2013). An auxin transport mechanism restricts positive orthogravitropism in lateral roots. Current biology : CB *23*, 817-822.

Roychoudhry, S., Del Bianco, M., Kieffer, M., and Kepinski, S. (2013). Auxin controls gravitropic setpoint angle in higher plant lateral branches. Current biology : CB *23*, 1497-1504.

S F Yang, a., and Hoffman, N.E. (1984). Ethylene Biosynthesis and its Regulation in Higher Plants. Annual Review of Plant Physiology *35*, 155-189.

Sakai, H., Hua, J., Chen, Q.G., Chang, C., Medrano, L.J., Bleecker, A.B., and Meyerowitz, E.M. (1998). ETR2 is an ETR1-like gene involved in ethylene signaling in Arabidopsis. Proc Natl Acad Sci U S A *95*, 5812-5817.

Sun, X.Z., Li, Y.X., He, W.R., Ji, C.G., Xia, P.X., Wang, Y.C., Du, S., Li, H.J., Raikhel, N., Xiao, J.Y.*, et al.* (2017). Pyrazinamide and derivatives block ethylene biosynthesis by inhibiting ACC oxidase. Nat Commun *8*.

Uga, Y., Sugimoto, K., Ogawa, S., Rane, J., Ishitani, M., Hara, N., Kitomi, Y., Inukai, Y., Ono, K., Kanno, N.*, et al.* (2013). Control of root system architecture by DEEPER ROOTING 1 increases rice yield under drought conditions. Nature genetics *45*, 1097-1102.

Vaseva, II, Qudeimat, E., Potuschak, T., Du, Y., Genschik, P., Vandenbussche, F., and Van Der Straeten, D. (2018). The plant hormone ethylene restricts Arabidopsis growth via the epidermis. Proc Natl Acad Sci U S A *115*, E4130-E4139.

Waidmann, S., Ruiz Rosquete, M., Scholler, M., Sarkel, E., Lindner, H., LaRue, T., Petrik, I., Dunser, K., Martopawiro, S., Sasidharan, R.*, et al.* (2019). Cytokinin functions as an asymmetric and anti-gravitropic signal in lateral roots. Nat Commun *10*, 3540.

Waite, J.M., and Dardick, C. (2021). The roles of the IGT gene family in plant architecture: past, present, and future. Curr Opin Plant Biol *59*.

Wen, X., Zhang, C., Ji, Y., Zhao, Q., He, W., An, F., Jiang, L., and Guo, H. (2012). Activation of ethylene signaling is mediated by nuclear translocation of the cleaved EIN2 carboxyl terminus. Cell Res *22*, 1613-1616.

Xiao, G., and Zhang, Y. (2020). Adaptive Growth: Shaping Auxin-Mediated Root System Architecture. Trends in plant science *25*, 121-123.

Yoshihara, T., and Spalding, E.P. (2017). LAZY Genes Mediate the Effects of Gravity on Auxin Gradients and Plant Architecture. Plant Physiology *175*, 959-969.

Zhu, Y., Li, H.J., Su, Q., Wen, J., Wang, Y.F., Song, W., Xie, Y.P., He, W.R., Yang, Z., Jiang, K.*, et al.* (2019). A phenotype-directed chemical screen identifies ponalrestat as an inhibitor of the plant flavin monooxygenase YUCCA in auxin biosynthesis. J Biol Chem *294*, 19923-19933.

Zurcher, E., Tavor-Deslex, D., Lituiev, D., Enkerli, K., Tarr, P.T., and Muller, B. (2013). A robust and sensitive synthetic sensor to monitor the transcriptional output of the cytokinin signaling network in planta. Plant Physiol *161*, 1066-1075.

FIGURE LEGENDS

Figure1. MBZ treatment perturbs root system architecture (RSA).

(A) 14-day-old Arabidopsis seedlings of grown on DMSO and MBZ (1 µM) plates.

(B) Quantification of GSA in (A). 15 LRs per seedling on DMSO plates, 12 LRs per seedling on MBZ plates, and 6 seedlings for each condition were used. Unpaired, two-tailed Student's t-tests was used for statistical analysis. **** $p < 0.0001$.

(C) 7-day-old seedlings on DMSO and MBZ (1 µM) plates.

(D) Quantification of primary root length (cm) in (B). 15-20 seedlings for each treatment were used. **** $p < 0.0001$.

(E) 14-day-old (upper panel) Arabidopsis seedlings on DMSO plates were transferred to MBZ (1 µM) plates, and 19-day-old (bottom panel) seedlings on MBZ (1 µM) plates were transferred to DMSO plates, followed by continuous scanning for 24 h.

(F) Changes of lateral root angle after plate transfer from DMSO to MBZ (red and yellow lines) or MBZ to DMSO (blue, purple lines) compared to timepoint 0.

(Scale bar: A, C, G, 1 cm; E, 5 mm.). Boxplots: Whiskers: min/max values; hinges: 25th to 75th percentile; mid-line: median.

Figure 2. MBZ treatment regulates the ethylene pathway.

(A) Gene ontology (GO) analysis upregulated genes (abs(log2) fold change > 1) from DEGs upon MBZ treatment in roots of 14-day-old Arabidopsis seedlings.

(B) Heatmap of DEGs involved in the ethylene pathway, which were detected to be differentially expressed upon MBZ treatment in the RNA-seq analysis. The left 4 columns of DMSO are data from 4 replicates of samples from DMSO (Mock) plates. The right 4 columns of MBZ are data from 4 replicates of samples from MBZ treatment plates. The heatmap was made online by heatmapper (http://heatmapper.ca/expression/), The cluster method is complete linkage. Color bar indicates the relative expression level.

(C-E) Venn diagrams showing differentially expressed genes in 3 h MBZ treatment and 3 h ACC treatment. All genes (FDR < 0.05; abs(log2) fold change > 1) (C), upregulated genes (FDR < 0.05; log2 fold change > 1) (D), downregulated genes (log2 fold change < -1) (E).

(F) Dot plots showing the most enriched GO terms with KS p-value < 0.05 from DEGs upon MBZ treatment in lateral root tips of 14-day-old seedlings.

(G-I**)** Representative images of lateral root tips of two-week-old plants in response to negative control, positive control and MBZ treatment using ethylene (*EIN3-GFP*)(G), auxin (*DR5v2-GFP*)(H), and cytokinin (*TCSn-GFP*)(I) reporter lines at 0 and 60 minutes of treatment.

(J**)** Relative fluorescent intensity of *EIN3-GFP* lateral root tips treated over a course of 4 h with DMSO, MBZ, and ACC.

(K**)** Relative fluorescent intensity of *DR5v2-GFP* lateral root tips treated over a course of 4 h with DMSO, MBZ, and IAA.

(L**)** Relative fluorescent intensity of *TCSn-GFP* lateral root tips treated over a course of 4 h with DMSO, MBZ, and tZ. 6 lateral roots for each treatment were used. Unpaired, two-tailed Student's t-tests were used to compare the data of MBZ or the corresponding positive controls to DMSO at each timepoint. *: p<0.05; **: p<0.01; ***: p<0.001.

Figure 3. MBZ induces ethylene responses and mimics ACC treatment.

(A) 4-day-old etiolated seedlings grown on MS, 10 µM ACC, DMSO, 10 µM MBZ plates. 20 seedlings were observed for each treatment.

(B-C) Quantification of hypocotyl length (B) and primary root length (C) of seedlings in (A). 20 seedlings for each treatment were used. **** p < 0.0001.

(D) Images of median longitudinal optical sections of primary root meristem and mature zone stained with propidium iodide (PI) of 4-day-old etiolated Col-0 on DMSO, 2.5 µM MBZ, and 10 µM ACC plates, 6-10 seedlings were observed for each treatment.

(E-F) Meristem length (E) and mature cell size (F) of seedlings in (D). 6-10 seedlings for each treatment were used. Different letters label significant different values (p<0.0001). One-way ANOVA and *post hoc* Tukey testing were used for statistical analysis in (E) and (F). (Scale bar: **A**, 5 mm; **D**, 100 µm.). Boxplots: Whiskers: min/max values; hinges: 25th to 75th percentile; mid-line: median.

Figure 4. MBZ acts downstream of ethylene biosynthesis.

(A) Quantification of ethylene production by GC-MS of 4-day-old etiolated seedlings of Col-0 in vials with DMSO, 10 µM MBZ, and 10 µM ACC medium. 100 seedlings for every vial, 4 biological replicates for each treatment, ND: not detectable.

(B) 6-day-old seedlings of Col-0, *etr1-1*, and *etr1-3* grown on DMSO and 1.2 µM MBZ plates. 20 seedlings were observed.

(C) Quantification of root length in (A). 20 seedlings were countified.

(D) 16-day-old seedlings of Col-0 and *etr1-1* grown on DMSO and 1.2 µM MBZ plates. 20 seedlings were observed.

(E) Quantification of GSA in (C). 20 seedlings were countified.

One-way ANOVA and *post hoc* Tukey testing were used for statistical analysis in b and d. Different letters label significant different values ($p<0.0001$). (Scale bar: **B**, **D**, 1 cm.) Boxplots: Whiskers: min/max values; hinges: 25th to 75th percentile; mid-line: median.

Figure 5. MBZ targets the ethylene signaling pathway.

(A) Diagram of ethylene signaling pathway.

(B) 7-day-old seedlings of Col-0, *ctr1-1*, and *ein2-5* grown on DMSO and 1.2 µM MBZ plates.

(C) Quantification of primary root length of seedlings in (B) 15-20 seedlings were quantified. Similar results were obtained from three biological replicates of the experiment.

(D) 19-day-old seedlings of Col-0 and *ctr1-1* grown on DMSO and 1.2 µM MBZ plates.

(E) Quantification of GSA of seedlings in (D). 10 seedlings were quantified. Similar results were obtained from three biological replicates of the experiment.

(F) 16-day-old seedlings of Col-0 and *ein2-5*, *ein3 eil1* grown on DMSO and 1.2 µM MBZ plates.

(G) Quantification of GSA of seedlings in (F). *dm* stands for *ein3 eil1* double mutants.

One-way ANOVA and *post hoc* Tukey testing were used for statistical analysis in **C**, **E**, and **G**. Different letters label significant different values ($p<0.0001$). (Scale bar: **B**, **D**, **F**,

1 cm.). Boxplots: Whiskers: min/max values; hinges: 25th to 75th percentile; mid-line: median.

Figure 6. MBZ inhibits CTR1 kinase activity.

(A) Sequence alignment of *hs*MAPK14 and CTR1-KD in Arabidopsis around 4 core amino acids (Highlighted by blue and pink frames) for MBZ binding.

(B) Molecular modeling of the interaction between MBZ (coppery) and CTR1-KD (silvery). In the left panel, the key residues that contribute to the binding with CTR1-KD were highlighted. The right panel showed the surface (gray) of the catalytic pocket of CTR1-KD.

(C) Western blot using Recombinant Anti-Thiophosphate ester antibody under different concentration of MBZ treatment. Left panel: CTR1-KD; Right panel: MAPK4. MBP is the substrate in both panels, MBZ concentration is 0, 10, and 100 µM as labeled in different reactions, [ATPγS]CTR1-KD: ATPγS binding CTR1-KD, [ATPγS]MAPK4: ATPγS binding MAPK4, MBP that obtained ATPγS from CTR1-KD or MAPK4, which is labeled as [ATPγS]MBP. Note: ATPγS: Adenosine 5'-(3-thiotriphosphate) tetralithium salt (Sigma, Cat# A1388)

(D) Coomassie blue staining of the gel shown in (C). CTR1: ~100 ng, MAPK4: ~1 µg. Myelin Basic Protein (MBP, a common kinase substrate, Sigma Cat. M1891): 2 µg, ATPγS: 1 mM. MBZ: 0, 10, or 100 µM. Arrows label the position of these bands on the gel.

Figure 7. Working model for MBZ action on ethylene signaling.

(A) Ethylene suppresses CTR1 activity to promote EIN2C translocation and activates ethylene signaling.

(B) MBZ inhibits CTR1 activity by binding to its kinase domain and promotes EIN2C translocation to activate the ethylene signaling.

Note: EIN2C: C-terminal of EIN2; ATP: Adenosine triphosphate; ADP: adenosine diphosphate; C2H4: ethylene; P: Phosphate group

Figure S1. MBZ treatment affects root growth and development.

(A) Chemical structure of MBZ.

(B-C) Root hair phenotype of 7-day-old seedlings on DMSO and 1 µM MBZ plates recorded by a scanner (B) or a microscope (C). 20 seedlings were observed on left panel and 10 seedlings were observed on right panel. (Scale bar: **B**, 13 mm; **C**, 1000µm)

Figure S2. Analysis of differentially expressed genes (DEGs) upon MBZ treatment.

(A-C) Venn diagrams showing differentially expressed genes in 4 h MBZ treatment in roots of 14-day-old green seedlings and published 4 h ethylene treatment in 3-day-old etiolated seedlings. All genes (FDR<0.05; abs(log2) fold change > 1) (A), upregulated genes (FDR<0.05; log2 fold change > 1) (B), downregulated genes (FDR<0.05; log2 fold change < -1) (C).

(D) Gene ontology (GO) analysis of upregulated genes (FDR<0.05; log2 fold change > 1) from DEGs upon MBZ treatment.

Figure S3. Etiolated seedling phenotypes in mutants of the ethylene pathway.

(A) 4-day-old etiolated seedlings of Col-0 and *etr1-3* grown on DMSO, 2.5 µM MBZ, and 10 µM ACC plates.

(B-C) Quantification of hypocotyl length (B) and root length (C) of seedlings in (A). 20 seedlings were quantified.

(D) 4-day-old etiolated seedlings of Col-0, *ctr1-1, ein2-5*, and *ein3 eil1* grown on DMSO, 2.5 µM MBZ, and 10 µM ACC plates.

(E-F) Quantification of hypocotyl length (E) and root length (F) of seedlings in **D**. 20 seedlings were quantified. Statistical analysis in **B, C** and **E, F** were done using unpaired, two-tailed Student's t-tests. P-values are indicated in the figure. (Scale bar: **A, D**, 1 cm). Whiskers: min/max values; hinges: 25th to 75th percentile; mid-line: median.

Figure S4. Alignment of CTR1-KD in Arabidopsis and MAPK14 in human.

(A) The structure alignment of *hs*MAPK14 (coppery) and CTR1-KD (celeste).

(B) The protein binding sites in *hs*MAPK14 (coppery) and CTR1-KD (periwinkle) with highlighted key residues.

(C) Sequence alignment of kinase domains. Key residues in MAPK14_human and CTR1-KD in Arabidopsis are indicated by red boxes.

(D) Phylogenetic analysis of kinases aligned in (C).

Figure S5. High concentrations or long-term treatment of MBZ induce phenotypes that go beyond ethylene induced effects.

(A) Confocal microscopy images of a root meristem of 4-day-old etiolated WT seedling grown on 10 µM MBZ plate.

(B) 38-day-old Col-0 plants grown on DMSO and 1.2 µM MBZ plates.

(C)14-day-old seedlings of Col-0 grown on increasing concentrations MBZ and ACC (0.1, 0.2, 0.4, 1, 2, 4, 10 µM) 20 seedlings were observed. Similar results were obtained from three biological replicates of the experiment. (Scale bar: **A**, 100 µm, **B**, **C**, 1 cm)

Table S1. The list of blast hits in Arabidopsis using the MAPK14_human sequence as BLASTP.

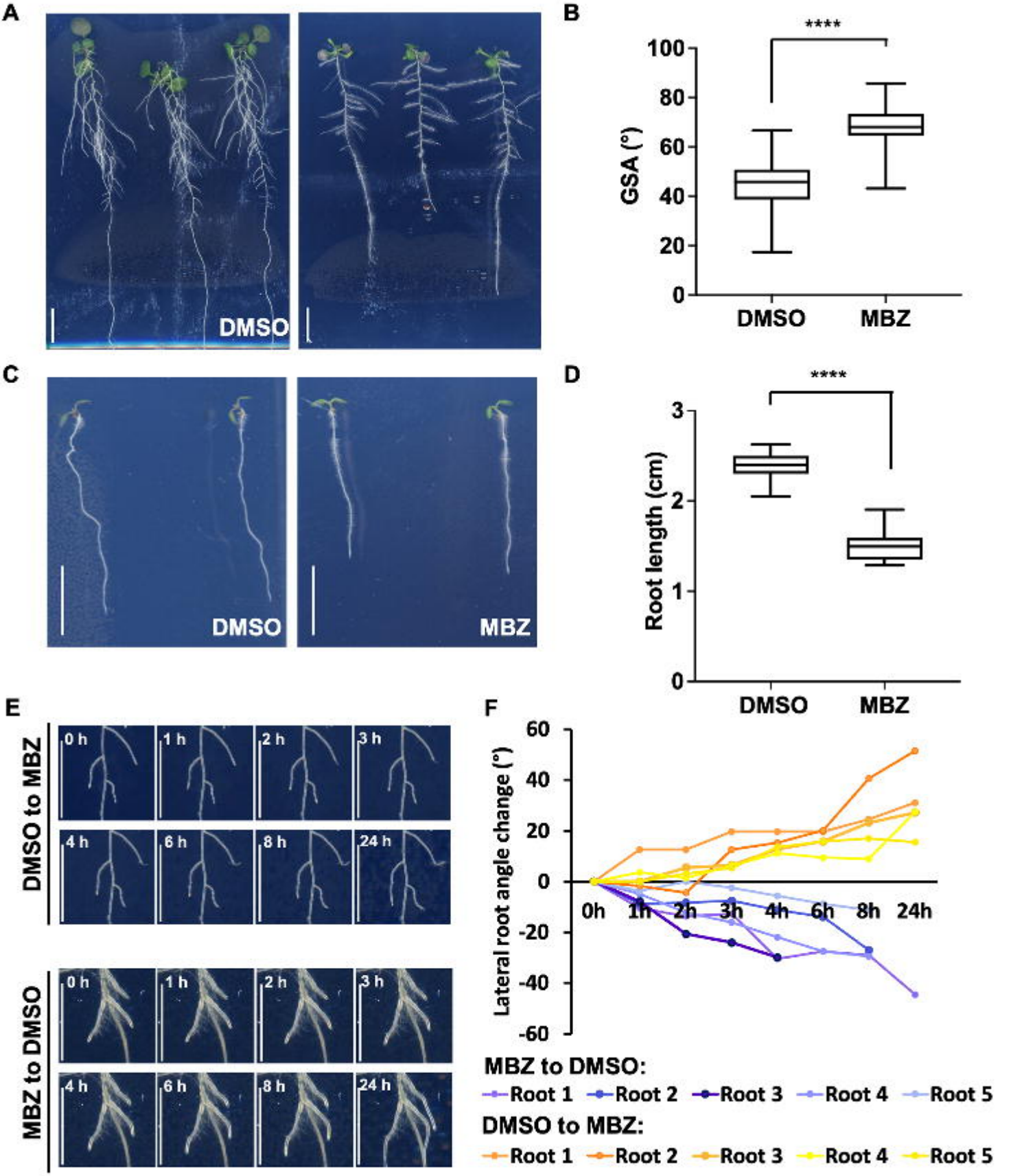

Figure 1. MBZ treatment perturbs root system architecture (RSA).

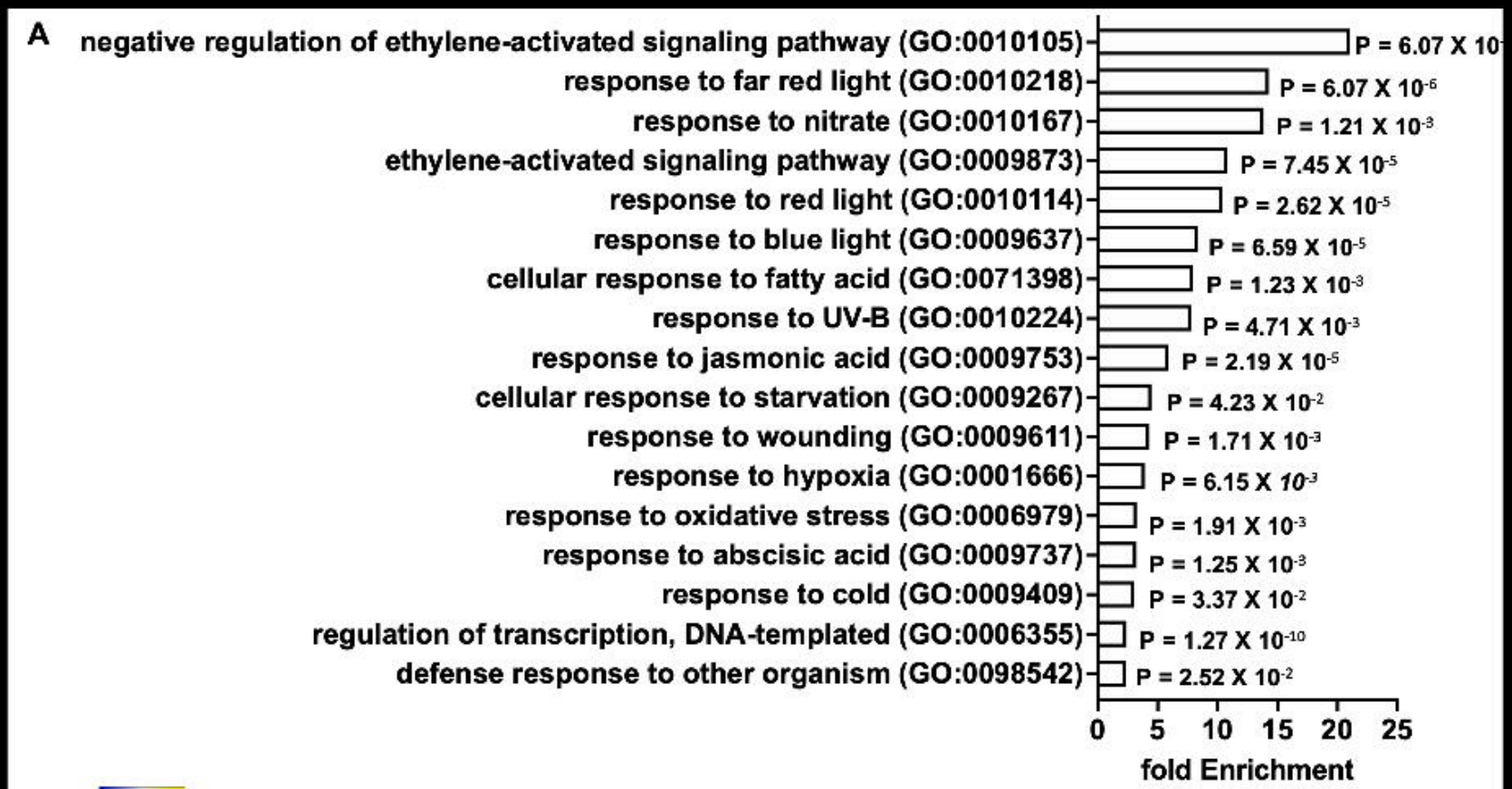

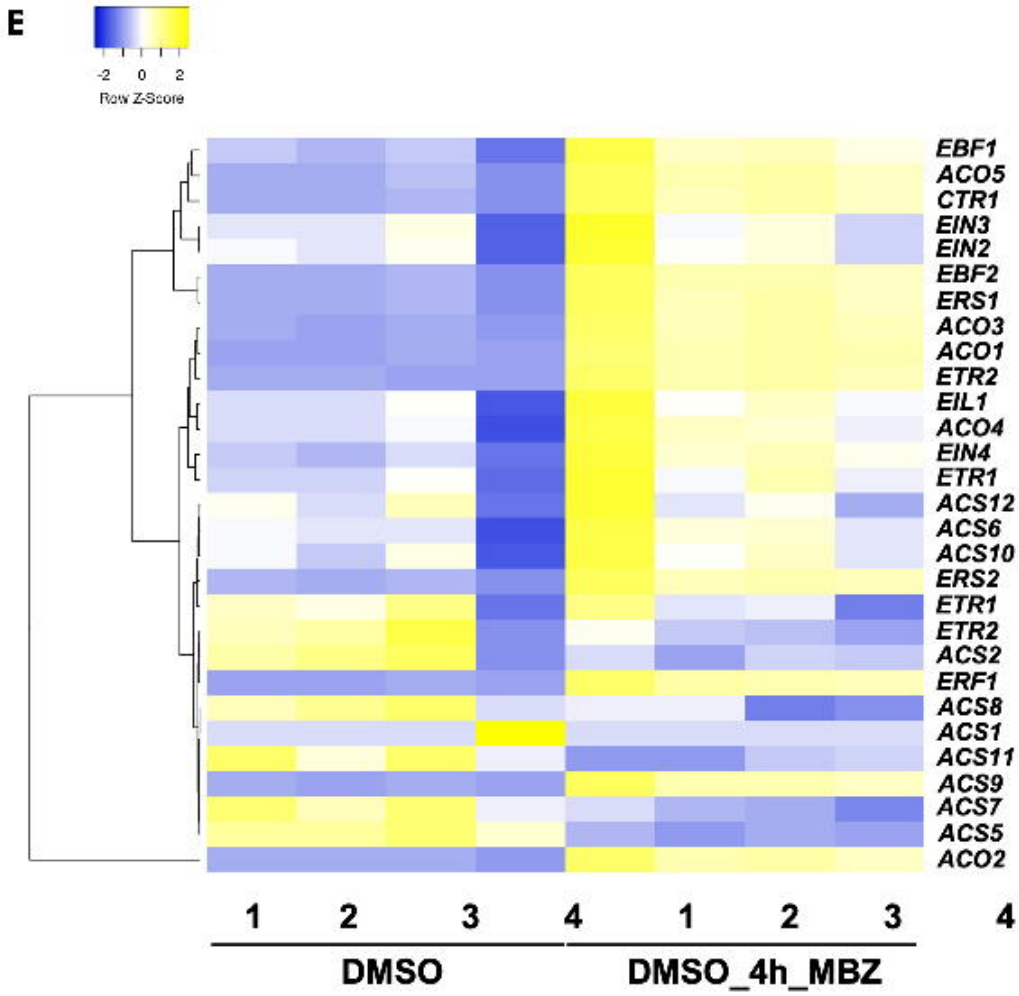

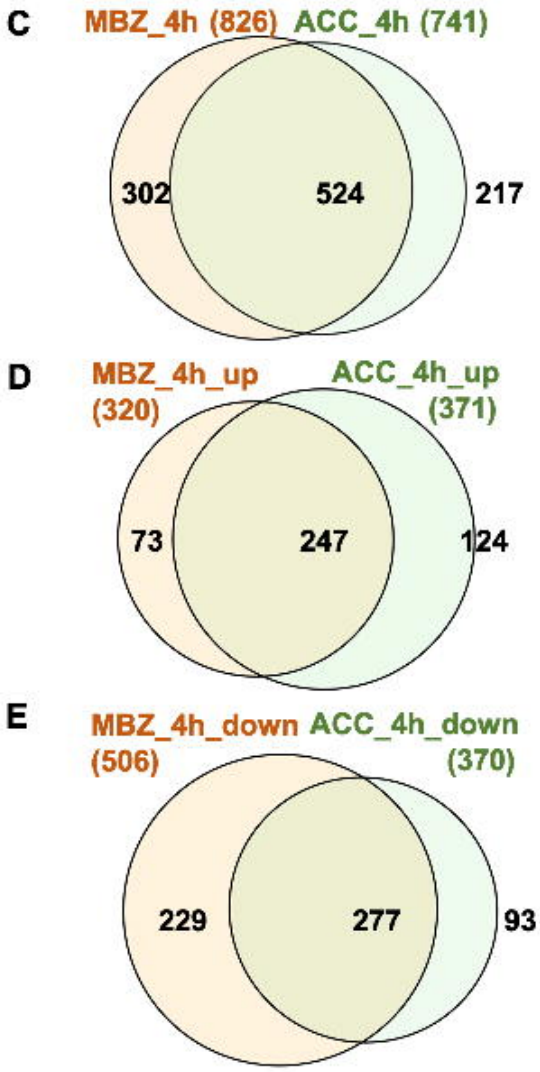

Figure 2. MBZ treatment regulates the ethylene pathway.

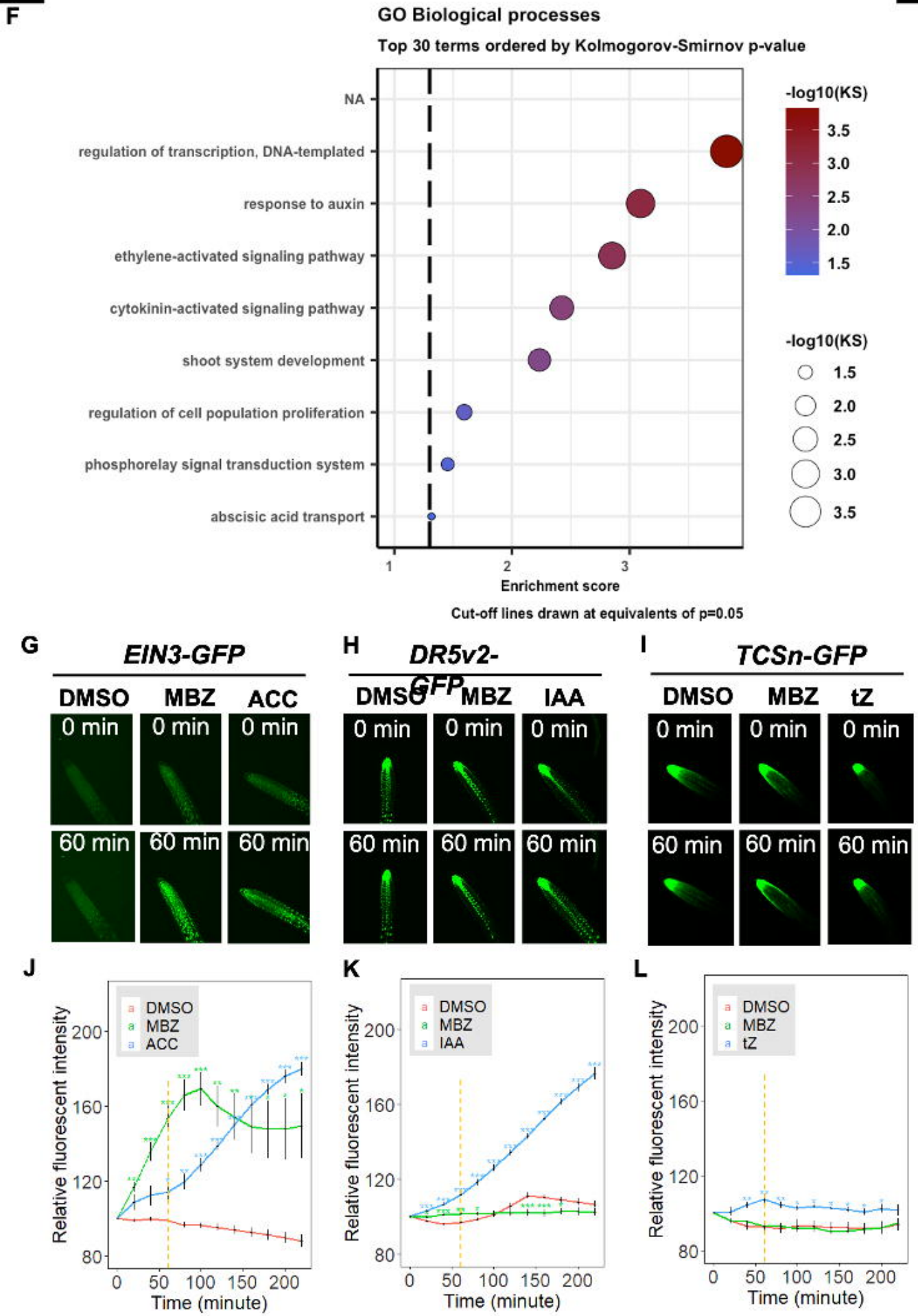

Figure 2. MBZ treatment regulates the ethylene pathway.

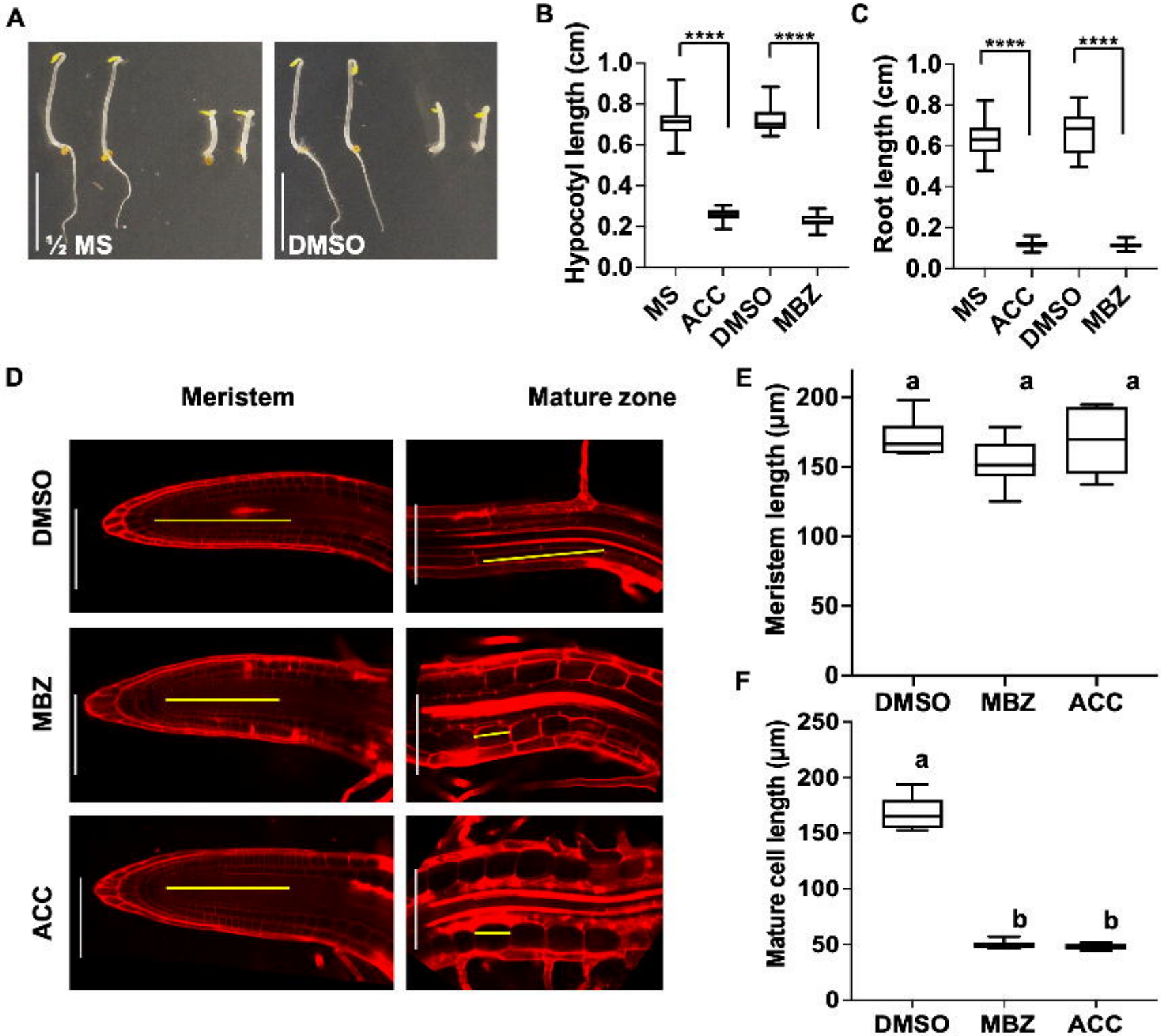

Figure 3. MBZ induces ethylene response and mimics ACC treatment

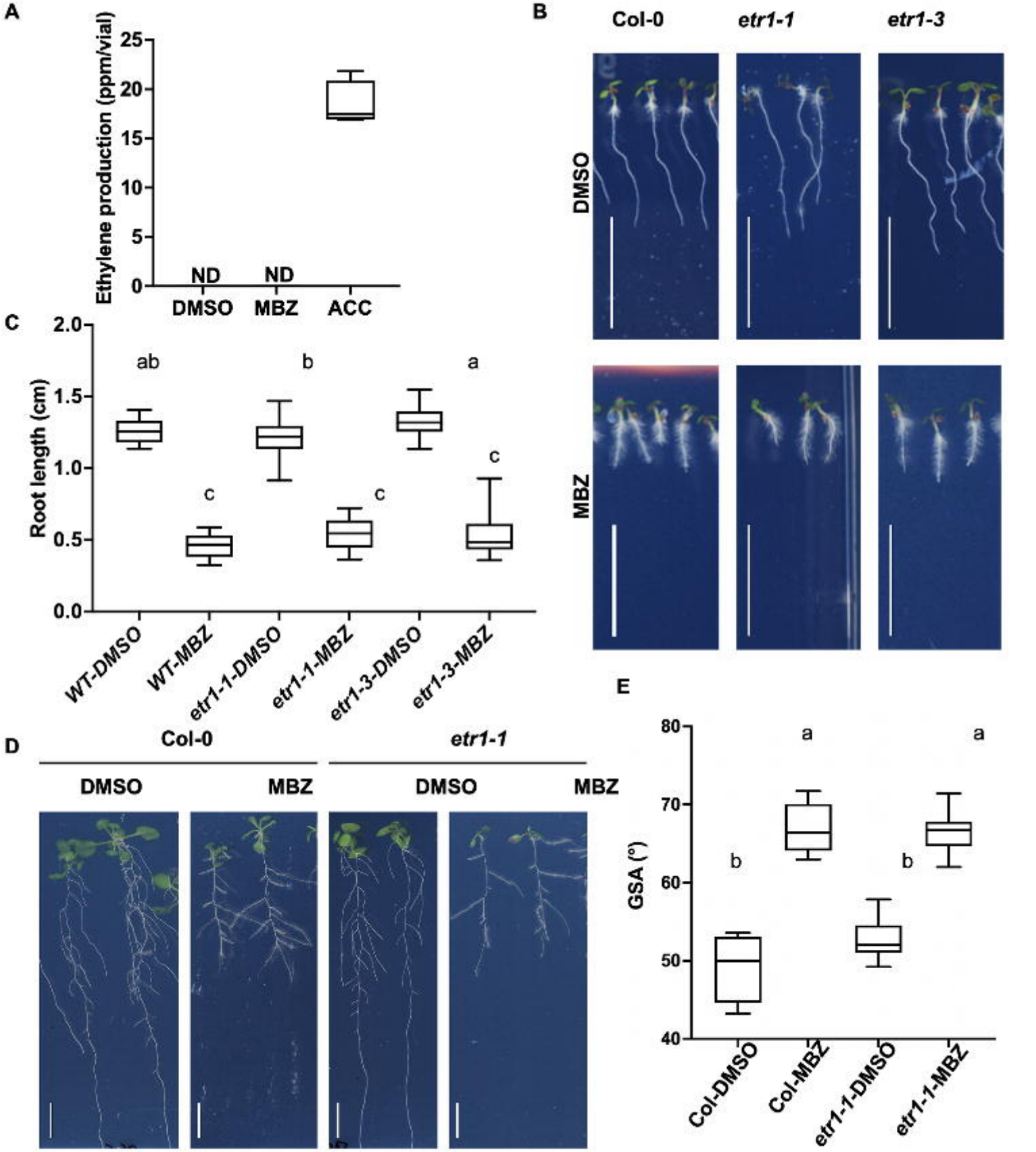

Figure 4. MBZ acts downstream of ethylene biosynthesis

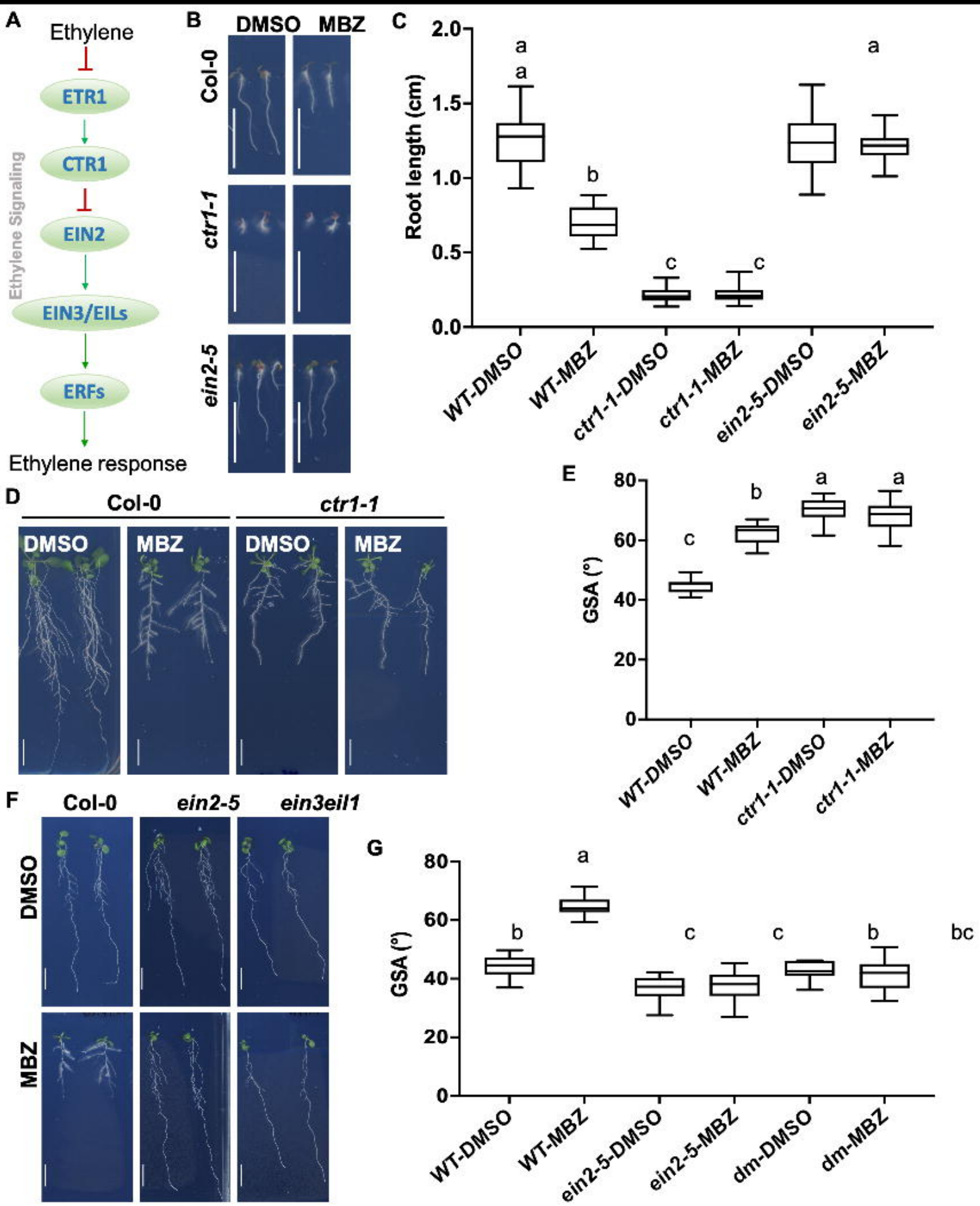

Figure 5. MBZ targets the ethylene signaling pathway

A

Identical aa | Similar aa

```
hsMAPK14 14   --NKTI-WEVPERYQNLSPVGSGAYGSVCAAFDTKTGLRVAVKKLSRPFQSIIHAKRTYR  70
AtCTR1  541   GDDMDIPWC---DLNIKEKIGAGSFGTVHRAEW--HGSDVAVKILMEQDFHAERVNEFLR 595

hsMAPK14 71   ELRLLKHMK-HENVIGLLDVFTPARSLEEFNDVYLVTHLMGAD----LNNIV-KCQKLTD 124
AtCTR1  596   EVAIMKRLR-HPNIVLFMGAVTQPP------NLSIVTEYLSRGSLYRLLHKSGAREQLDE 648

hsMAPK14 161  DCELKILDFGLARHTDDEM---TGYVATRWYRAPEIMLNW----MHYNQTVDIWSVGCIM 213
AtCTR1  687   KYTVKVCDFGLSRLKASTFLSSKSAAGTPEWMAPEVLRDE-----PSNEKSDVYSFGVIL 741
```

B

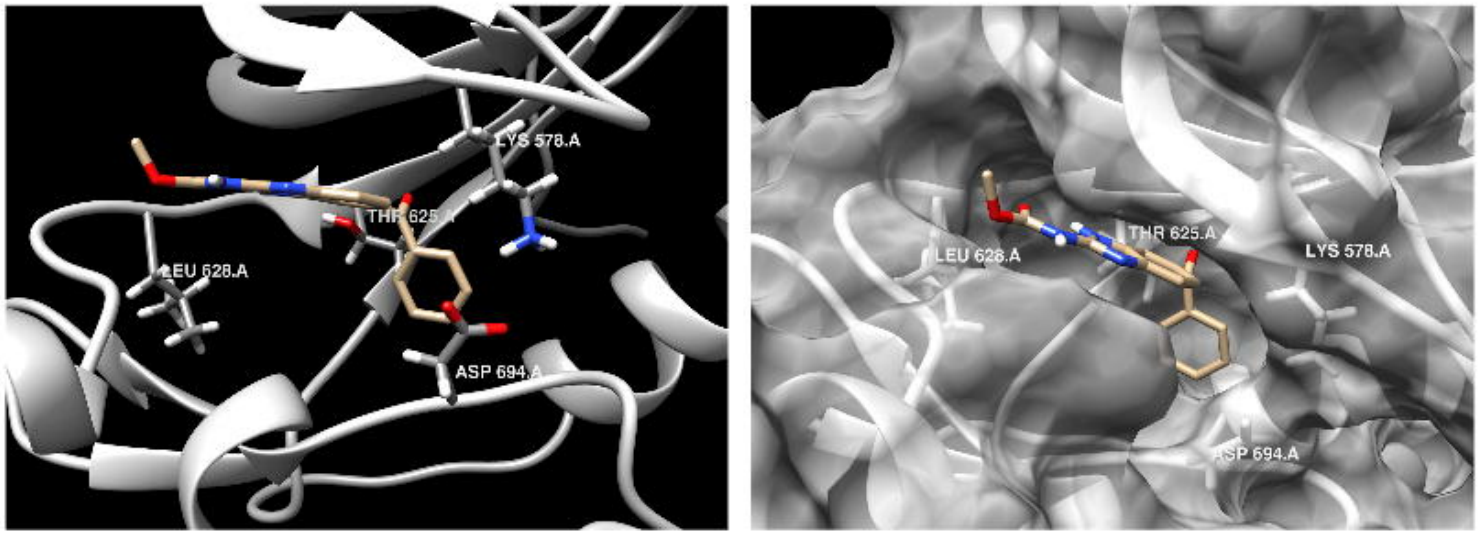

C

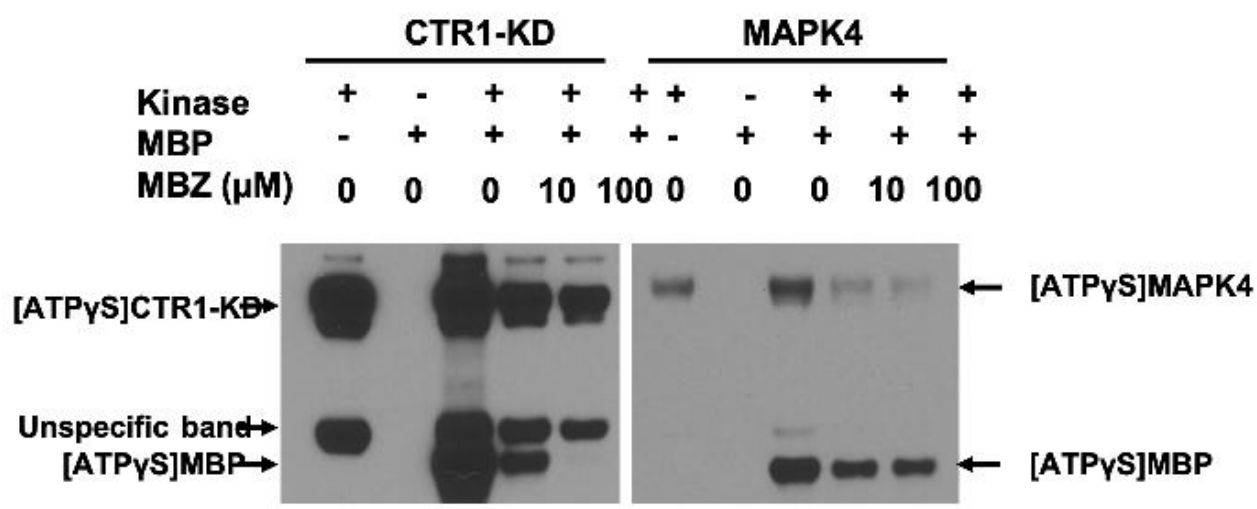

D

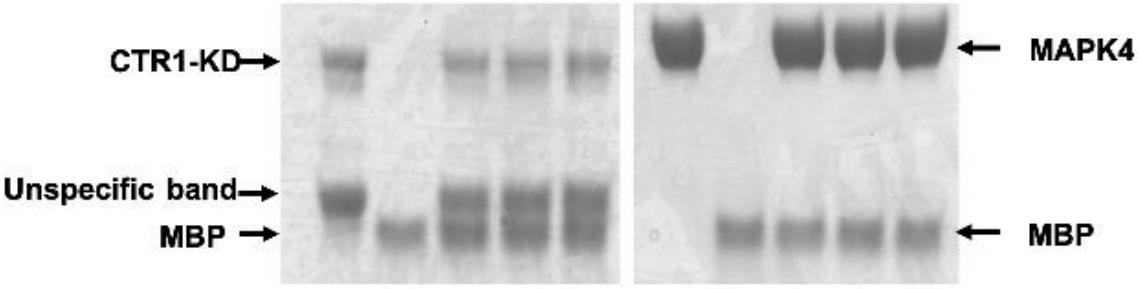

Figure 6. MBZ inhibits CTR1 kinase activity

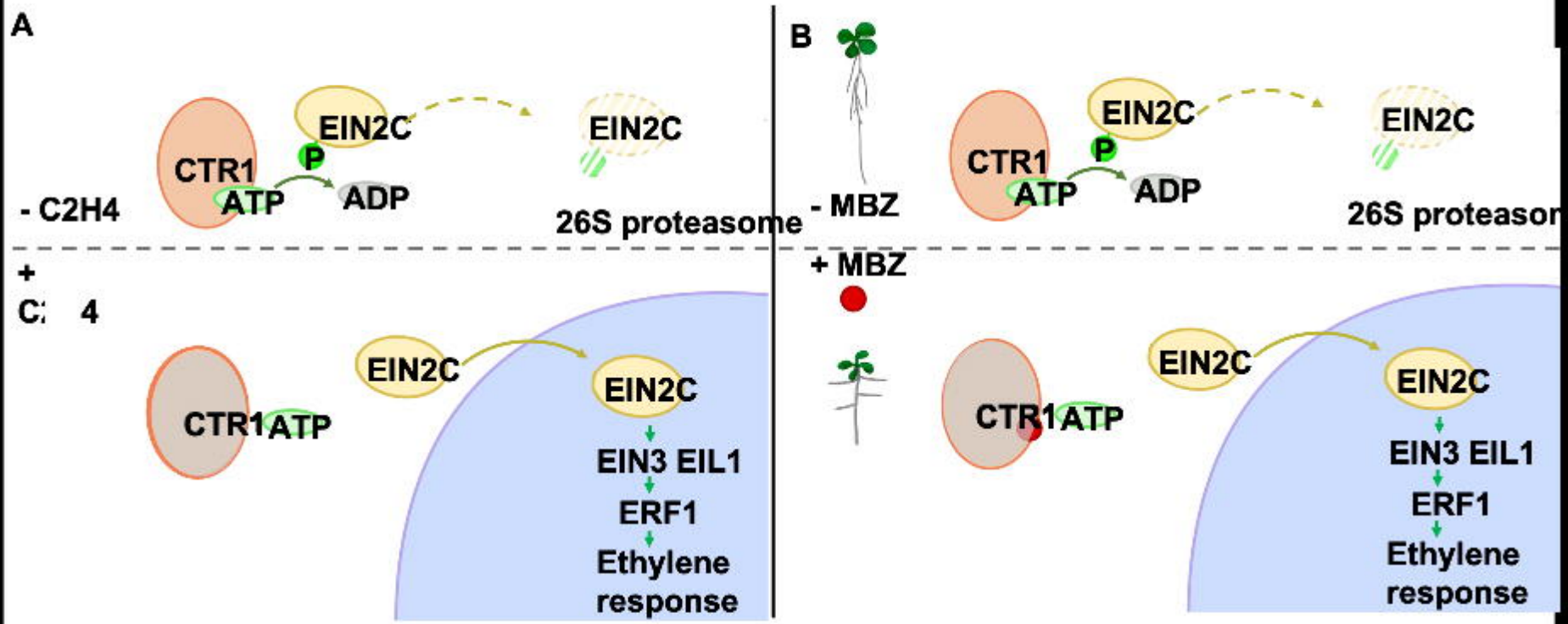

Figure 7. Working model for MBZ action on ethylene signaling

A

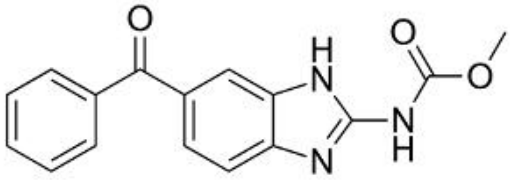

Mebendazole (MBZ)

B

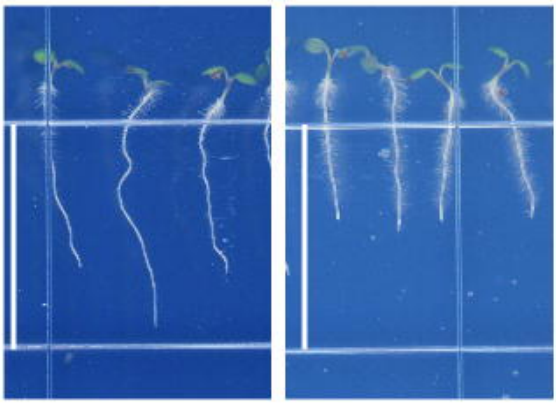

C

Figure S1. MBZ treatment affects root growth and develop

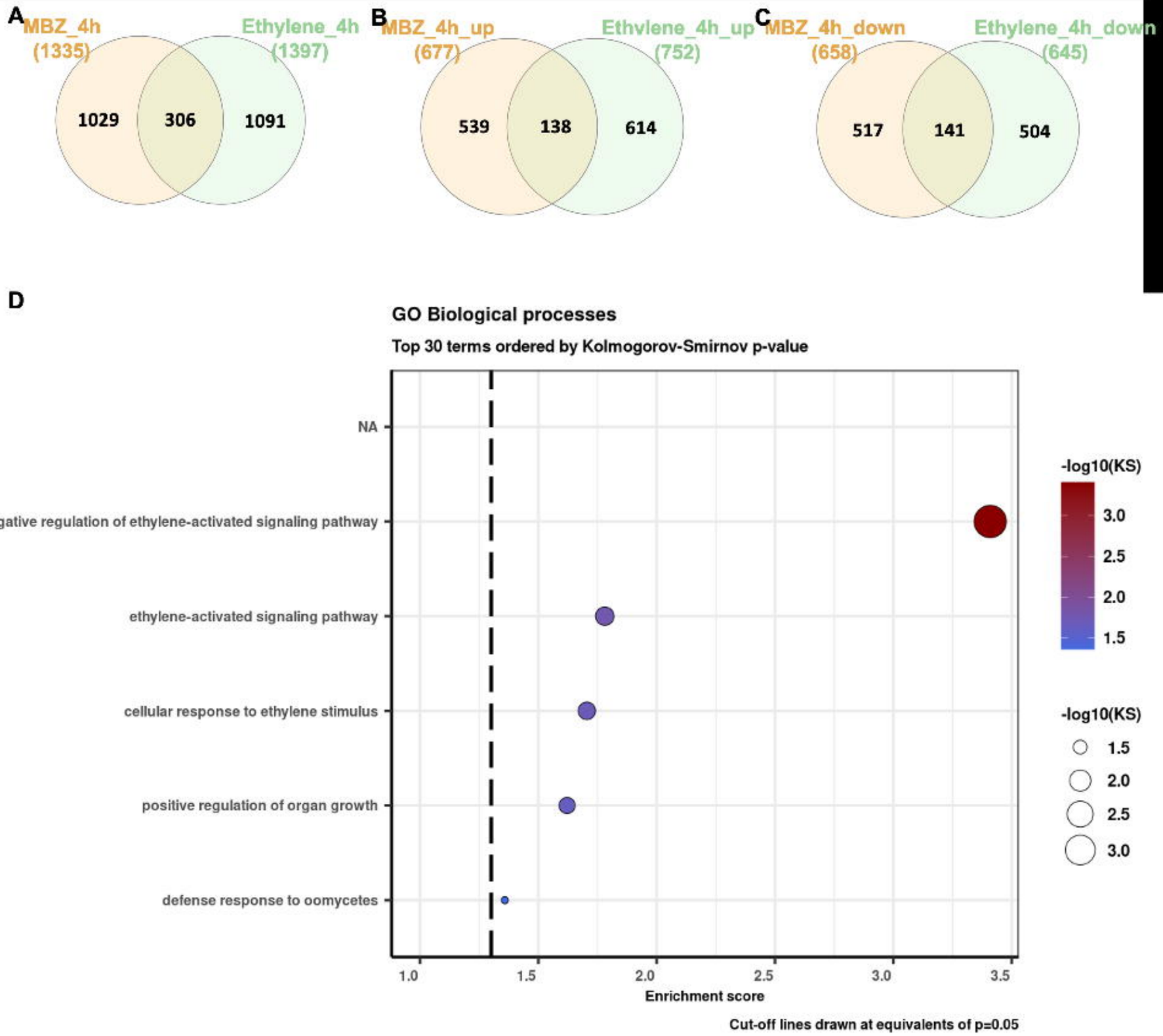

Figure S2. The analysis of differentially expressed genes (DEGs) by MBZ treatment.

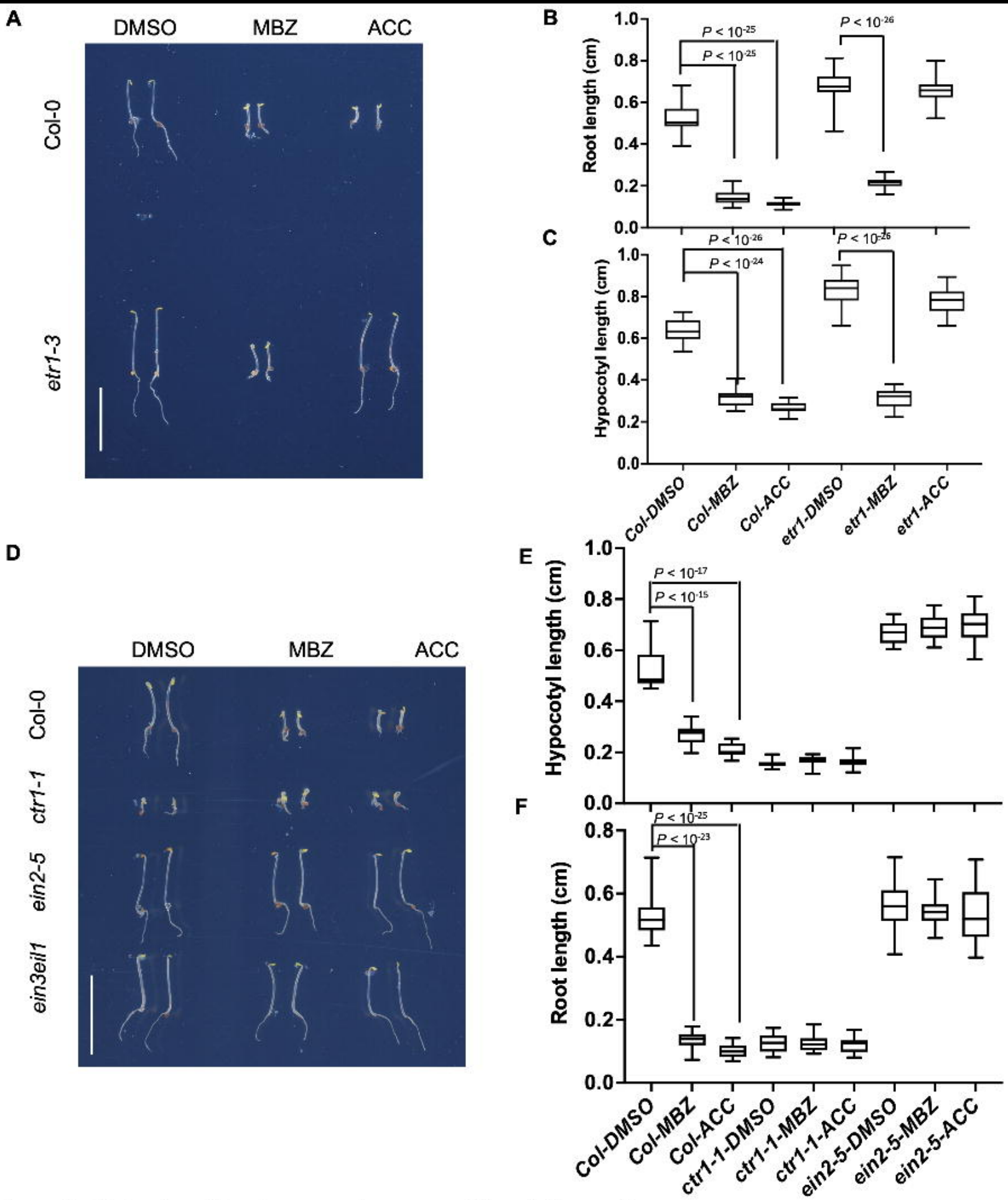

Figure S3. Etiolated seedling phenotypes in mutants of the ethylene pathway.

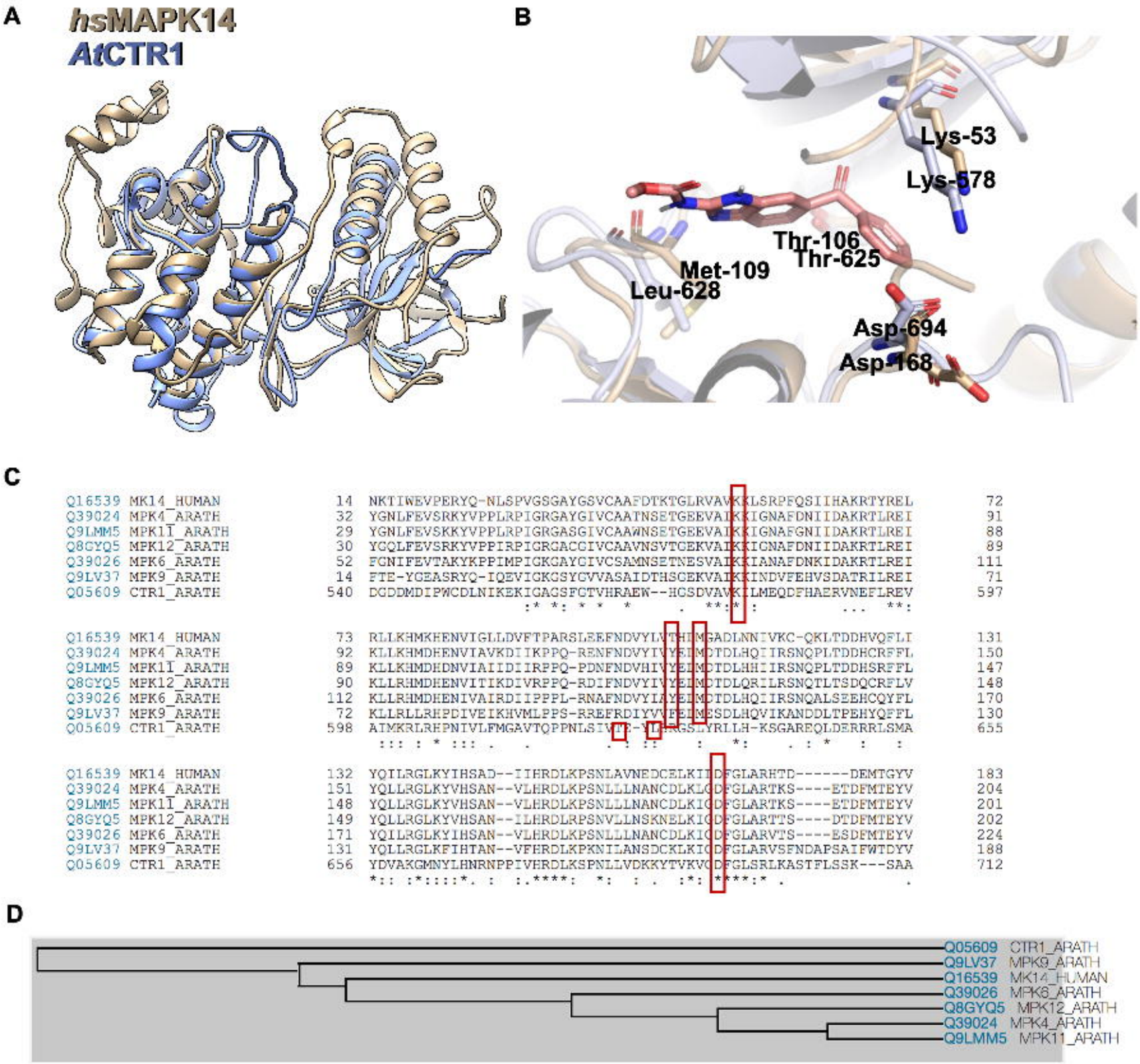

Figure S4. Alignment of *At*CTR1-KD and *hs*MAPK14

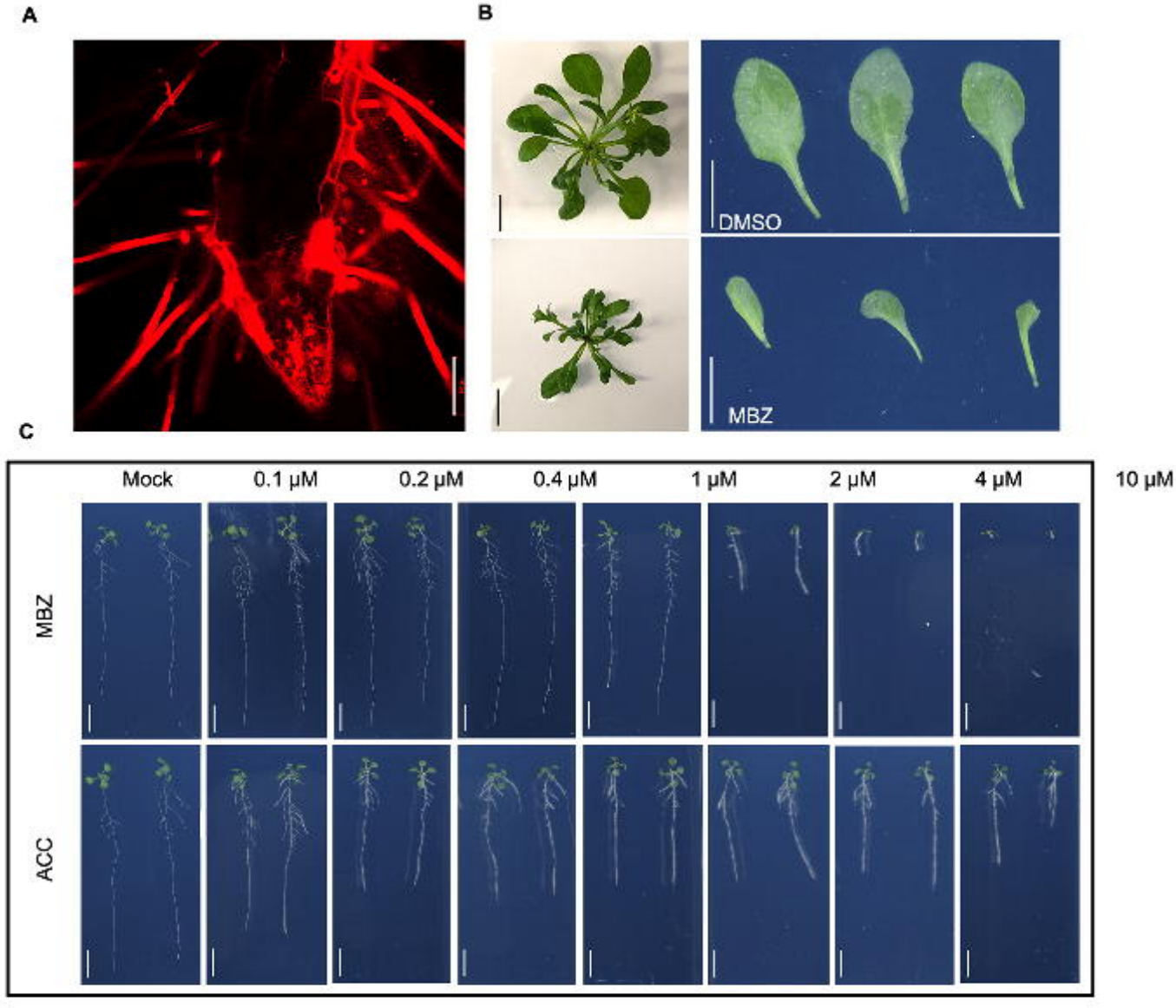

Figure S5. High concentrations or long-term treatment of MBZ induce phenotypes that go beyond ethylene induced effects

Table S1. The list of blast hits in Arabidopsis using the MAPK14_human sequence as BLASTP

JVD8454701R-Alignment-Descriptions

Description	Scientific Name	Max Score	Total Score	Query Cover	E value	Per Ident	Acc. Len	Accession
MAP kinase 4 [Arabidopsis thaliana]	Arabidopsis thaliana	348	348	93%	3E-117	51.18	376	NP_189306.1
mitogen-activated protein kinase 4 [Arabidopsis thaliana]	Arabidopsis thaliana	348	348	93%	3E-117	51.18	376	ABR01146.1
mitogen-activated protein kinase 4 [Arabidopsis thaliana]	Arabidopsis thaliana	345	345	93%	8E-117	50.80	376	ABR01146.1
MAP kinase [Arabidopsis thaliana]	Arabidopsis thaliana	345	345	93%	9E-117	50.80	376	BAA34667.1
mitogen-activated protein kinase 4 [Arabidopsis thaliana]	Arabidopsis thaliana	344	344	93%	1E-116	50.80	376	ABT40162.1
unnamed protein product [Arabidopsis thaliana]	Arabidopsis thaliana	340	340	95%	3E-115	47.71	376	VYS02239.1
MPK6 [Arabidopsis thaliana]	Arabidopsis thaliana	339	339	95%	5E-115	47.71	376	CAA38194.1
MAP kinase 11 [Arabidopsis thaliana]	Arabidopsis thaliana	337	337	93%	6E-114	49.71	366	NP_001117210.1
unnamed protein product [Arabidopsis thaliana]	Arabidopsis thaliana	337	337	93%	6E-114	49.71	366	CAA07942.1
MAP kinase 5 [Arabidopsis thaliana]	Arabidopsis thaliana	337	337	95%	6E-114	47.43	376	NP_567378.4
unnamed protein product [Arabidopsis thaliana]	Arabidopsis thaliana	336	336	95%	2E-113	49.84	376	CAD53345.1
MAP kinase [Arabidopsis thaliana]	Arabidopsis thaliana	335	335	95%	3E-113	49.55	376	BAA34666.1
mitogen-activated protein kinase 3 [Arabidopsis thaliana]	Arabidopsis thaliana	335	335	95%	3E-113	49.55	376	NP_190150.1
MAP kinase [Arabidopsis thaliana]	Arabidopsis thaliana	330	330	95%	3E-111	49.57	376	BAA34668.1
mitogen-activated protein kinase 12 [Arabidopsis thaliana]	Arabidopsis thaliana	329	329	92%	9E-111	49.26	372	NP_182131.2
mitogen-activated protein kinase 13 [Arabidopsis thaliana]	Arabidopsis thaliana	329	329	92%	3E-110	49.29	408	NP_001182606.1
Mitogen-activated protein kinase 8 [Arabidopsis thaliana]	Arabidopsis thaliana	329	329	99%	3E-108	49.84	366	6YH1_A
Crystal structure of Arabidopsis thaliana MPK6 [Arabidopsis thaliana]	Arabidopsis thaliana	329	329	99%	3E-108	49.84	372	6CH4_A
unnamed protein product [Arabidopsis thaliana]	Arabidopsis thaliana	329	329	92%	3E-108	49.31	366	VYS02634.1
MAP kinase 6 [Arabidopsis thaliana]	Arabidopsis thaliana	329	329	95%	4E-108	49.84	366	NP_181907.1
MAP kinase 10 [Arabidopsis thaliana]	Arabidopsis thaliana	329	329	92%	4E-108	49.31	366	NP_191526.1
unnamed protein product [Arabidopsis thaliana]	Arabidopsis thaliana	329	329	92%	5E-108	49.31	366	CAA03975.1
MPK13 [Arabidopsis thaliana]	Arabidopsis thaliana	323	323	92%	8E-106	49.31	366	CAP05405.1
unnamed protein product [Arabidopsis thaliana]	Arabidopsis thaliana	321	321	92%	2E-107	49.22	366	CAD53262.1
MAP kinase [Arabidopsis thaliana]	Arabidopsis thaliana	318	318	95%	2E-106	49.29	372	CAB51417.1
Protein kinase superfamily protein [Arabidopsis thaliana]	Arabidopsis thaliana	317	317	92%	4E-106	47.79	366	NP_001032496.1
unnamed protein product [Arabidopsis thaliana]	Arabidopsis thaliana	316	316	92%	4E-106	47.79	366	CAD53120.1
mitogen-activated protein kinase homolog 3 [Arabidopsis thaliana]	Arabidopsis thaliana	316	316	95%	7E-106	49.84	376	NP_564726.1
ATMPK1 [Arabidopsis thaliana]	Arabidopsis thaliana	315	315	93%	2E-105	49.33	372	BAA03535.1
unnamed protein product [Arabidopsis thaliana]	Arabidopsis thaliana	315	315	93%	3E-105	49.33	372	CAA19627.1
AT1G10210 [Arabidopsis thaliana]	Arabidopsis thaliana	315	315	93%	3E-105	49.33	372	BAH19911.1
mitogen-activated protein kinase 1 [Arabidopsis thaliana]	Arabidopsis thaliana	315	315	93%	3E-105	49.33	372	NP_001031317.1
mitogen-activated protein kinase 14 [Arabidopsis thaliana]	Arabidopsis thaliana	315	315	93%	3E-105	49.04	361	NP_199363.1
ATMPK2 [Arabidopsis thaliana]	Arabidopsis thaliana	315	315	95%	4E-105	49.39	372	BAA03536.1
unnamed protein product [Arabidopsis thaliana]	Arabidopsis thaliana	313	313	95%	1E-104	49.01	361	CAA07688.1
MPK14 [Arabidopsis thaliana]	Arabidopsis thaliana	311	311	95%	8E-104	44.70	361	CAD46458.1
MAP kinase 6-CT [Arabidopsis thaliana]	Arabidopsis thaliana	310	310	81%	9E-104	50	337	AB226416.1
MAP kinase 7 [Arabidopsis thaliana]	Arabidopsis thaliana	310	310	95%	2E-103	48.71	366	NP_179409.1
MPK7 [Arabidopsis thaliana]	Arabidopsis thaliana	310	310	95%	2E-103	48.71	366	CAP11026.1
MAP Kinase [Arabidopsis thaliana]	Arabidopsis thaliana	309	309	95%	4E-103	50.43	354	AAB51003.1
unnamed protein product [Arabidopsis thaliana]	Arabidopsis thaliana	310	310	91%	4E-103	48.49	366	CAD52215.1
unnamed protein product [Arabidopsis thaliana]	Arabidopsis thaliana	309	309	95%	5E-103	48.71	366	CAA39469.1
MAP kinase 11 [Arabidopsis thaliana]	Arabidopsis thaliana	307	307	78%	2E-102	52.58	348	NP_001182112.1
MAP kinase [Arabidopsis thaliana]	Arabidopsis thaliana	306	306	95%	1E-101	48.56	366	BAA34670.1
unnamed protein product [Arabidopsis thaliana]	Arabidopsis thaliana	310	310	93%	3E-99	49.12	716	CAD53301.1
mitogen-activated protein kinase 12 [Arabidopsis thaliana]	Arabidopsis thaliana	297	297	93%	3E-99	51.23	394	NP_001166735.1
mitogen-activated protein kinase 10 [Arabidopsis thaliana]	Arabidopsis thaliana	297	297	91%	7E-99	42.77	567	NP_197409.1
Unknown protein [Arabidopsis thaliana]	Arabidopsis thaliana	287	287	91%	1E-92	42.77	567	AAL32807.1
unnamed protein product [Arabidopsis thaliana]	Arabidopsis thaliana	287	287	91%	9E-92	42.77	568	CAD53215.1
MAP kinase [Arabidopsis thaliana]	Arabidopsis thaliana	276	276	75%	6E-90	50	360	BAD 95376.10
putative MAP kinase [Arabidopsis thaliana]	Arabidopsis thaliana	271	271	93%	3E-87	49.6	431	AAK92464.1
MPK15 [Arabidopsis thaliana]	Arabidopsis thaliana	274	274	92%	1E-88	41.89	575	CAP17697.1
MAP kinase 19 [Arabidopsis thaliana]	Arabidopsis thaliana	268	268	91%	3E-86	42.18	429	NP_001028986.1
MAP kinase 15 [Arabidopsis thaliana]	Arabidopsis thaliana	272	272	92%	4E-86	41.86	575	NP_568370.3
MPK9 [Arabidopsis thaliana]	Arabidopsis thaliana	269	269	92%	1E-84	42.15	568	CAP16797.1